

Spacecraft Propulsion and Design Challenge

Phobos Orbiter Mission Design: MomenTUM

1st Beatriz Mas Sanz

*Chair of Space Propulsion and Mobility
Technical University of Munich
Munich, Germany
ge86san@mytum.de*

2nd Marta Pelivan

*Chair of Space Propulsion and Mobility
Technical University of Munich
Munich, Germany
marta.pelivan@tum.de*

3rd Julian Schmid

*Chair of Space Propulsion and Mobility
Technical University of Munich
Munich, Germany
juli.schmid@tum.de*

4th Sven J. Steinert

*Chair of Space Propulsion and Mobility
Technical University of Munich
Munich, Germany
0000-0003-4424-670X*

Abstract—The target of this design challenge is, to develop a propulsion system concept that can provide the sufficient performance to send a spacecraft to Phobos with an Ariane 62 rocket as its launch system. For this, different concepts are compared in a variety of trade-offs. Finally, a system that uses a bipropellant as well as an electric propulsion system is chosen and worked out in detail to prove, that this concept can satisfy the given requirements of the launcher, the mission and the propulsion system itself.

Index Terms—Mars, Phobos, quasi-satellite orbit, bipropellant, chemical propulsion, electrical propulsion

I. INTRODUCTION

The study presented in this report focuses on the preliminary design of the propulsion system for a proposed mission to Phobos, one of the moons of Mars. The primary objective of this mission is to study the origin, together with the physical and chemical composition of Phobos, through the deployment of a surface probe.

The feasibility of the mission will be ensured by designing a propulsion system that can safely and efficiently transport the spacecraft to Phobos, maintain a Quasi-Satellite Orbit (QSO) around the moon for a minimum of two years, and provide sufficient power and propulsion for the surface probe to conduct its scientific experiments. The spacecraft is planned to be launched on a dedicated Ariane 62 rocket from Kourou between 2026-2029, and it will be de-orbited into the Martian atmosphere at the end of its mission.

The report will begin by describing the trajectory to reach Phobos. This will be followed by the presentation of the proposed concept for the propulsion system, along with a detailed explanation of the trade-offs leading to the final concept, its components and how it addresses the challenges of the mission.

Overall, the study performed in this report aims to present a feasible preliminary design that can help ensure the success of the mission.

II. WORKFLOW

In this section, the workflow design process of the spacecraft and specifically the spacecraft propulsion system is introduced. This is shown in Figure 1. In it, a continuous iteration process is presented to ensure, that an optimized spacecraft configuration can be reached. The main mechanism in this process is a closed loop between the mission analysis software General Mission Analysis Tool (GMAT) and the self-developed MATLAB (The Mathworks, Inc.) scripts `dV_calc.m`, `mass_design.py` and `pressure_temp_sim.m`. Results, such as a propulsion subsystem schematic, technical drawings of the system and different budgets for mass, propellant and delta v can be drawn from this process.

A. GMAT

The General Mission Analysis Tool (GMAT) is used to compute the trajectory and simulate the mission in space and time. Hereby the mission was first implemented impulsive, then with finite chemical burns and ultimately with additional finite electric burns in `MomenTUM_finite.script`. As an output of this simulation, a result file `result.txt` is created, holding certain events by their timestamp and fuel level as well as burn-times and key-variables of the mission. This rather long file is shortened to the most important lines by a small script `cleaning.py` into `result_clean.txt`. Additionally the distance to Phobos is outputted by GMAT and plotted by `plot.py`.

B. dv Script

The delta v script `dV_calc.m` is a program written in MATLAB. Its function is to take a given spacecraft dry mass, as well as the thrust and ISP of the engine used in the maneuvers, together with the dedicated burn-times from GMAT per maneuver. These values are then transformed into the respective delta v and propellant mass of each maneuver via the Tsiolkovsky rocket equation [1].

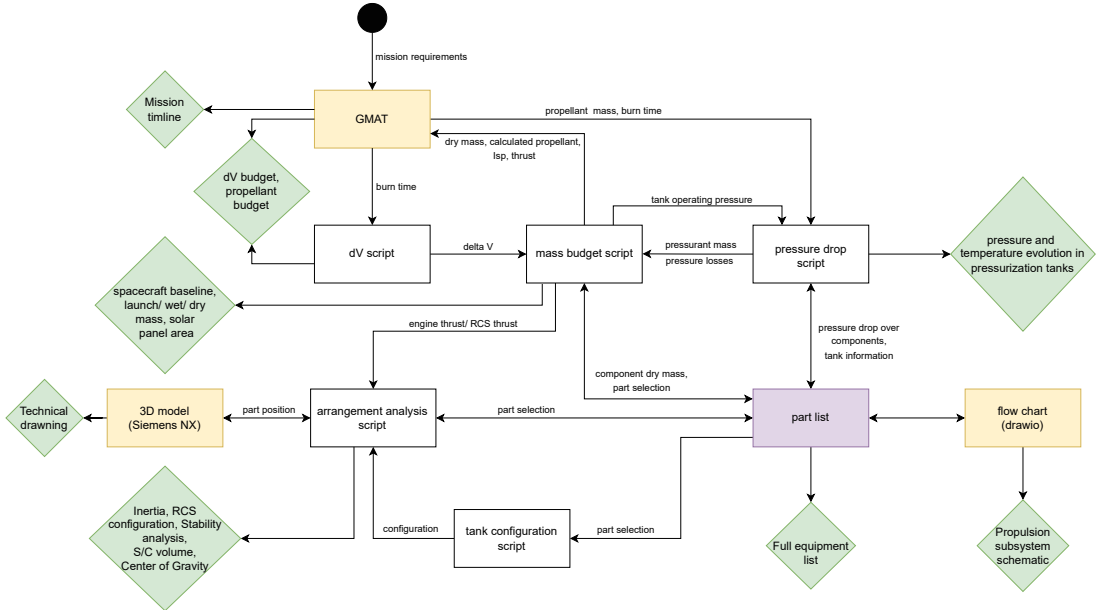


Fig. 1. Flowchart of workflow

C. Mass Budget Script

To compute the launch mass of the spacecraft as well as the solar array size and the engine performance data, a mass budget script `mass_design.py`, written in MATLAB, is used. Here, the delta v's and the pressurant mass are needed as an input, while especially the spacecraft dry mass and engine performance is inserted back into GMAT as an output of this script. In this script, the ESA margin philosophy [2] is respected.

D. Pressure Script

The amount of pressurant required for the mission is calculated using the MATLAB pressure script `pressure_temp_sim.m`. The required inputs for the tool are the `result_clean.txt` file coming from GMAT transformed to a `.xlsx` file, as well as the pressurant and propellant tank characteristics (volumes and mean operating pressures). The outputs of this script are:

- the total helium mass within the whole system at the beginning of operation, which is fed back to GMAT.
- the amount of helium within both pressurant and propellant tanks throughout the maneuvers.
- the pressure and temperature changes of helium within the pressurant and propellant tanks during the maneuvering time.

E. Arrangement Analysis Script

The spacecraft's configuration is determined by the arrangement analysis script `arrangement_analysis.m`, written in MATLAB. In this script, the orbital stability criteria for the spacecraft are matched with the spacecrafats geometrical layout and placement of the individual internal parts. This then results in a shape which directly influences the placement of

the reaction control system (RCS). By the correct placement of the RCS thrusters, a combined main-engine placement offset and misalignment can be compensated, resulting in a resilient spacecraft design. A 3D model can then be derived from this configuration and fed back to indicate if the internal parts fit within the restricted volume. The spacecraft's volume, the shifting center of gravity (CoG) and the moments of inertia are an output of this analysis which can then be compared to the requirements of the launch vehicle [3].

III. MISSION ANALYSIS AND OVERALL SPACECRAFT

A. Mission Requirements

The mission requirements form the baseline of the design process and are directly given in the design challenge [4].

TABLE I
MISSION REQUIREMENTS [4]

| Mission Requirements | |
|----------------------|---|
| Req. ID | Statement |
| MIS.001 | The system shall send a satellite to Phobos which will release a surface probe to Phobos ,one of the moons of Mars, to study its origin as well as its physical and chemical composition. |
| MIS.002 | The satellite shall be launched by a dedicated Ariane 62 |
| MIS.003 | The total system mass shall not exceed 2600 kg. |
| MIS.004 | The launch date shall lay between 2026 and 2029. |
| MIS.005 | The system shall reach an orbit around Phobos (Quasi-Satellite Orbit (QSO)) for a minimum of 2 years to study Phobos from space and to serve as a relay for the surface probe. |
| MIS.006 | At end of life (EOL) the spacecraft shall be de-orbited into the martian atmosphere (40km altitude at periapsis). |

B. Basic Mission Trajectory

For a transit to Mars, multiple launch windows are possible within the required launch frame of 2026 to 2029 (MIS.004). The most interesting opportunities are the energy minima Type 2 transfers in 2026 [5] where the required characteristic energy (C3) and arrival excess speed are particularly low. In order to offer a safety margin in case of any delays, the second most optimal window, starting at 31.10.2026 was chosen which takes place before the most optimal one at 6.11.2026. So in a case of emergency the launch date can be prospered while still being able to fly the mission with the same hardware.

The trajectory starts by its carrier, an Ariane 62 (MIS.002) and its ejection on its outgoing asymptote. However, the mission launch opportunity requires $9.144 \text{ km}^2/\text{s}^2$ of C3 where the Ariane 62 can only supply a infinity velocity of 2.5 km/s ($6.25 \text{ km}^2/\text{s}^2$ C3). Therefore the first maneuver is performed to match the required C3, when the spacecraft is leaving the influence of earth. Next, a trajectory correction maneuver (TCM) is performed to target the arrival at Mars precisely. When arriving at Mars, a Mars orbit insertion (MOI) is performed to reduce the spacecraft access velocity to a high elliptical orbital velocity. When crossing Phobos orbital plane, an inclination change is done near to the spacecrafts apoapsis followed by a raise of its periapsis to intersect with Phobos orbit. To match the point in time where Phobos and the spacecraft align, a parking orbit is created where after one round-trip, Phobos is matched with a deceleration burn where now its orbital parameters are similar to achieve a quasi satellite orbit. For the required delta v to perform orbital maintenance, literature values for this case have been used as $\frac{1.16}{8.23} \text{ m/s}$ delta v per day [6] and the mission duration MIS.005 plus margin. Ultimately as MIS.006 requires, the spacecraft is deorbited into the martian atmosphere through a deceleration burn at its apoapsis. The full set of delta v magnitudes for this impulsive trajectory and its V,N,B vector components are listed in table II corresponding to `MomenTUM_impulsive.script`.

TABLE II
REQUIRED DELTA V FOR IMPULSIVE MANEUVERS

| Maneuver Name | Magn. [m/s] |
|-----------------------|-----------------|
| C Match C3 | 509.350 |
| C TCM | 34.553 |
| C MOI | 751.782 |
| C Match INC | 13.153 |
| E Raise Peri | 35.660 |
| E Parking Insertion | 197.507 |
| E Match Phobos | 640.000 |
| E Orbital Maintenance | 104.950 |
| E EOL | 561.664 |
| Total | 2848.619 |

| V | N | B |
|---|---|---|
| x | | |
| x | x | x |
| x | | |
| | x | |
| x | | |
| x | | |
| x | | |
| x | x | x |
| x | | |

C. Propulsion System Trade-off

To analyze which propulsion system combination shall be used for this mission, the following trade-off, depicted in Table III is conducted. The objective is to select the configuration with the minimum launch mass, which is calculated by the mass budget script. The mission delta v used in this comparison originates from a finite chemical implementation of the impulsive trajectory `MomenTUM_biprop_only.script`. The maneuvers Raise Peri to EOL are considered done electrically in a mixed system. In this analysis, if a maneuver is performed with an electric engine, the delta v is doubled because of the high uncertainty in regard to the continuous thrust maneuvers. In this simplified case, only the biprop-electric and the biprop propulsion system fulfil MIS.003 and stay below the 2600 kg capability of the launcher [3]. Since the biprop-electric system has the lowest launch mass and the doubling of the delta V for the electrical maneuvers is assumed conservatively high, the lightest propulsion system is expected to be the combination of a bipropellant and electric propulsion. A more detailed comparison between the bipropellant only and the biprop-electric system can be found in the Appendix A.

TABLE III
PROPULSION SYSTEM TRADE-OFF

| Propulsion System Trade-off | | | | | |
|-----------------------------|-----------------|--------|----------|-------------------|----------|
| Propulsion System | Biprop Electric | Biprop | Electric | Monoprop Electric | Monoprop |
| Total Mission dV [m/s] | 4698.2 | 3277.5 | 6555.0 | 4698.2 | 3277.5 |
| Launch Mass [kg] | 2124.4 | 2128.3 | 2878.3 | 3022.8 | 6949.7 |

D. Advanced Mission Trajectory

To apply the selected bipropellant and electric system, the trajectory has to be adapted. For the bipropellant section, the general approach of maneuvers can be kept, since their burn-times are comparably short. Besides the C3 maneuver, which has no time constrains, only the MOI critically spreads over a longer range of space and time as seen in Figure 2.

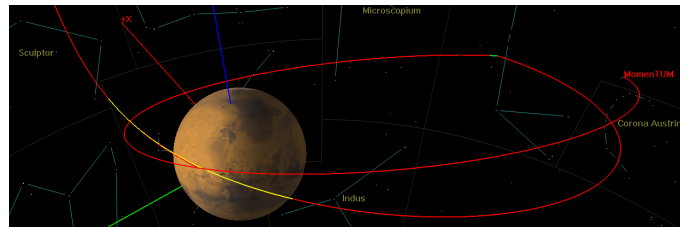


Fig. 2. Chemical maneuvers: MOI, Match INC, Raise Peri min

After the inclination change and raising the periapsis to a minimum, the maneuvers are carried out by the electric propulsion in a different approach. The first electric section is the circularization of the orbit through a loop of burns by true anomaly which can be seen in figure 3 where yellow sections represent thrust arcs. The over-raise in periapsis comes for the

benefit of drastically reduced flight-time and the over-raising is therefore a compromise of minimal delta v and flight-time.

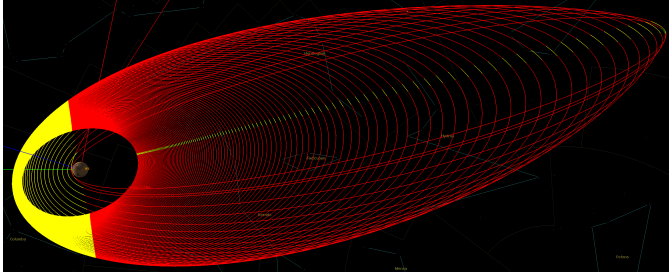


Fig. 3. Electric maneuver: Circularization

From there on, the electric thruster continuously fires to spiral down and approach Phobos. The very low eccentricity of Phobos is capitalized on here, so that a matching can be achieved from a circular spiral. To match the intersection with Phobos correctly in time, the spiraling is paused (displayed green in Figure 4) before its spiraling achieves a semi major axis of 9378.8 km and therefore a matching orbital period.

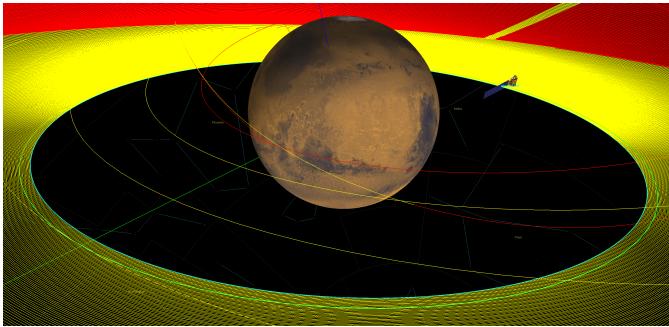


Fig. 4. Electric maneuver: Spiral Down Match

The Orbital Maintenance is assumed as in the impulsive section and its corresponding fuel mass is deducted. The EOL maneuver is also a loop of thrust arcs that decelerate the spacecrafts around its apoapsis, marked by true anomaly which can be seen in Figure 5. Hereby the assumption of 10 times the thrust equals to $\frac{1}{10}$ of the nominal burn-time was made to reduce computation time. This concludes the finite simulation of the selected bipropellant electrical system carried out in the GMAT script `MomenTUM_finite.script`.

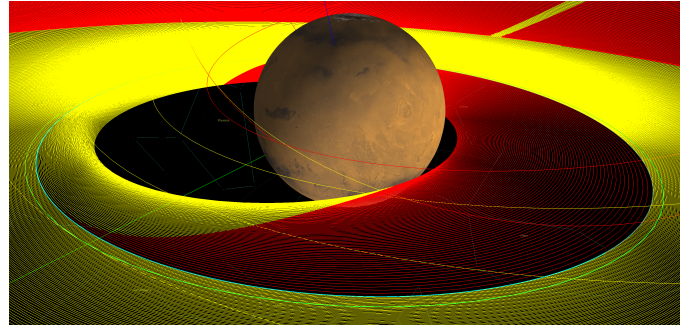


Fig. 5. Electric maneuver: EOL

E. *deltaV Budget*

As a result of the now fully specified trajectory and its finite simulation, the maneuver delta vs and burn times are given precisely in Table IV below.

TABLE IV
DELTAV BUDGET

| Maneuver Name | Type | [m/s] | [s] |
|---------------------|--------------------|-----------------|-------------------|
| C3 | finite | 516.868 | 2155.85 |
| TCM | finite | 1.395 | 5.35 |
| MOI | finite | 850.981 | 2858.31 |
| Match INC | finite | 14.550 | 42.44 |
| Raise Peri min | finite | 4.515 | 13.13 |
| Total Chemical | | 1388.308 | 5075.07 |
| Circularize | finite | 713.753 | 10164236.2 |
| Spiral Down Match | finite | 831.526 | 11334710.2 |
| Orbital Maintenance | stochastic | 104.950 | |
| EOL | finite, assumption | 708.395 | 9035872.4 |
| Total Electric | | 2358.624 | 30534818.8 |
| Total | | 3746.932 | 30539893.9 |

An more in depth overview of the mission is put together in the mission timeline in Table XXVIII that marks all states by a timestamp and their associated spacecraft values.

F. *Mass Budget*

The mass budget of the final spacecraft is depicted in Table V. It is generated by the mass budget script and lists all subsystems and propellants with their respective masses and margins. These margins are based on the ESA margin philosophy [2]. While most subsystem masses are already fixed for the mission, the STR and PWR subsystem need to be calculated via to following equations [4]. Regarding the STR subsystem, Equation 1 is used, while for the PWR subsystem, Equation 2 shall be applied. In case of the CPROP and EPROP subsystem, commercial parts are chosen to form the subsystems total mass. For the launch adapter, the PLA6 1194 is used which can be found in the user's manual of the

Ariane 62 [3]. In this budget, the dry mass is stated with the integrated Phobos surface probe, which is dropped in a later mission phase. This is because the harness and structural mass has to be sized for the probe as well, which then needs to be included. As a result, the dry mass is not a constant value over the whole mission.

$$m_{STR} = 0.0224 \cdot m_{wet} + 27.823 \quad (1)$$

$$m_{PWR} = 0.0758 \cdot P_{Earth} + 37.741 \quad (2)$$

TABLE V
MASS BUDGET

| SC Mass Budget | | |
|-------------------------------------|--------|---------------|
| System | Margin | Mass [kg] |
| AOGNC | 40.0 | |
| COM | 25.0 | |
| CDH | 15.0 | |
| CPROP | 126.9 | |
| EPROP | 45.4 | |
| INS | 50.0 | |
| MEC | 55.0 | |
| PWR | 398.6 | |
| STR | 73.9 | |
| TC | 15.0 | |
| Probe | 20.0 | |
| Harness | 10% | 86.6 |
| Dry Mass | | 951.3 |
| System Margin | 20% | |
| Dry Mass incl. System Margin | | 1141.6 |
| CPROP Fuel Mass | | 736.0 |
| CPROP Fuel Margin | 2% | 15.0 |
| CPROP Pressurant Mass | | 3.5 |
| CPROP Pressurant Mass Margin | 2% | 0.1 |
| EPROP Fuel Mass | | 162.7 |
| EPROP Fuel Mass Margin | 2% | 3.3 |
| Total Wet Mass | | 2062.4 |
| Launch Adapter | | 85.0 |
| Total Launch Mass | | 2147.4 |

G. Spacecraft Baseline

As a result of the mass budget, the spacecraft baseline design can be derived, which is shown in Table VI. In it, the chosen main components of the individual subsystems are displayed together with some key data. While the mass and the propulsion components, together with the heating system, are a direct optimized result of the iteration process between GMAT, the delta v budget, mass budget and pressure drop script, some other components are chosen on the basis of the Ice Giants mission from ESA [7]. The Phobos surface probe as a payload can be traced back to MIS.001 in Table I. Especially the space frame design is chosen to keep the placement of the propulsion system components flexible.

TABLE VI
SPACECRAFT BASELINE

| Spacecraft Baseline Design | |
|---------------------------------|---|
| Mass (incl. 20% sys. margin) | Dry mass: 1141.6 kg Chemical propellant mass (excl. margin): 751.3 kg Electrical propellant mass (excl. margin): 166.0 kg Wet mass: 2062.4 kg |
| Payload | Phobos surface probe Phobos imager |
| Propulsion | 1x main bipropellant thruster (450 N) 12x RCS thruster (12 N) 2x pressurant tank (40 l) 1x bipropellant tank (331 l) 2x bipropellant tank (198 l) 1x electric thruster (0.090 N) 2x noble gas tank (60 l) |
| AOGNC | 1x coarse rate sensor 2x navigation cameras 2x IMUs 2x star trackers 4x reaction wheels (+ RCS thrusters) |
| Communications | X-band uplink/downlink Ka-band downlink |
| Power | 2x solar array (2m x 7.5m) Power Processing Unit (PPU) + internal batteries |
| Data Handling | Redundant On-Board Computing (OBC) capability + storage |
| Structures | Space frame design |
| Thermal | MLI insulation blankets Heating system within the pressurant tanks |

IV. CHEMICAL PROPULSION SYSTEM

A. Chemical Propulsion System Requirements

The chemical propulsion system requirements in Table VII are derived from the mission requirements in Table I.

TABLE VII
PROPULSION SYSTEM REQUIREMENTS

| Propulsion System Requirements | |
|--------------------------------|--|
| Req. ID | Statement |
| CPROP.001 | The propulsion system shall provide the necessary thrust and delta v, required to perform the foreseen mission manoeuvres. |
| CPROP.002 | The propulsion system shall provide torques to compensate the main engine misalignments and for all other attitude and orbit control maneuvers, including safe-mode operation and reaction wheel off loading, as required by mission planning. |
| CPROP.003 | The subsystem shall have inhibits against critical failures leading to personnel hazard (e.g. while handling the spacecraft) |
| CPROP.004 | The propulsion system shall include single failure tolerant measurement of the propellant pressure. |
| CPROP.005 | The propulsion system shall provide means to isolate potential external leakages and/or failures of thruster flow control valves. |
| CPROP.006 | The propulsion system shall include access points (valves) for filling and draining the propulsion system on ground. |
| CPROP.007 | All components within the propulsion system shall be TRL9. |
| CPROP.008 | As many components as possible within the chemical propulsion system shall be of european origin. |

B. Assumptions

For the chemical propulsion system design the assumptions listed in Table VIII were used for the calculations.

TABLE VIII
ASSUMPTIONS

| Assumptions | |
|-------------|---|
| 1 | The overall ISP for the bipropellant engine is assumed to be an average between the main engine and RCS thrusters weighed by their thrust |
| 2 | The power required at Mars was scaled with respect to the power requirement in Earth using the inverse square law. |

C. Chemical System Trade-offs

The initial system trade-offs in Section III-C resulted in the selection of a bipropellant chemical subsystem over monopropellant. The application of this subsystem as part of an upper stage engine with low thrust range (< 40 kN) leads to the selection of a pressure fed cycle [4]. A dual-mode bipropellant system was disregarded since the bipropellant engine is relevant during the initial high-thrust phase of the mission, and the flexibility of switching to low-thrust, high-specific impulse propulsion is already provided by the electric propulsion subsystem.

Two main trade-off's were conducted for the bipropellant chemical subsystem design: the thruster selection process and the tank configuration.

The thruster selection was driven by requirements derived from the mission analysis calculations, which define a required thrust higher than 400 N, and a longest burn time of around 3000 s. The following thrusters were considered: Ariane S400-12, Ariane S400-15, NAMMO LEROS 2b and Aerojet Rocketdyne R-4D-15 HiPAT™. All these options fit the mission analysis requirements regarding thrust range, ISP, and oxidizer to fuel ratio. The Aerojet thruster was dismissed due to its US origin (CPROP.008). With the remaining European thrusters, the driver of the trade-off was the launch mass, which resulted the lower for the selected thruster: Ariane S400-15, as shown in Table IX [8].

TABLE IX
BIPROPELLANT MAIN THRUSTER TRADE-OFF

| Thruster | Launch mass [kg] | Thrust [N] | Burn Time [s] | ISP [s] |
|----------------|------------------|------------------|---------------|---------|
| Ariane S400-12 | 1584.494 | 340 to 440 [420] | 3960 | 318.000 |
| Ariane S400-15 | 1578.371 | 342 to 440 [425] | 6600 | 321.000 |
| NAMMO LEROS 2b | 1584.663 | 367 to 456 [420] | 6600 | 319.500 |

Nominal values in []

The selected propellant combination is Monomethylhydrazine (MMH) and mixed oxides of nitrogen (MON-3). The fuel is defined by the thruster specification. With respect to the oxidizer, the thruster enabled using Nitrogen Tetroxide (NTO), MON-1 or MON-3. MON was selected over NTO due to its lower sensitivity to temperature fluctuations and the higher availability of European tanks with demonstrated

compatibility. MON-3 was chosen over MON-1 because it has a lower vapor pressure, making it easier to handle and safely store before and during the mission.

A further trade-off determined number of propellant tanks required. Figure 6 shows the options considered, whereby the propellant tanks are from Ariane Group and the pressurant tanks from MT Aerospace (CPROP.007 and CPROP.008).

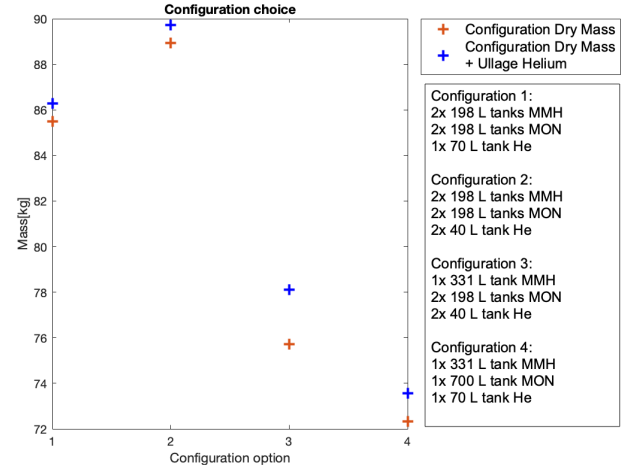


Fig. 6. Bipropellant Tanks Configuration Trade-off

The lightest option is configuration 4, however later stability analysis explained in Section VI-B proved it unsuitable. Therefore, the next lightest and thus selected configuration includes one 331 l MMH tank, two 198 l MON tanks and 2 40 l helium tanks.

The rest of the subsystem is developed around the selected thruster and tank configuration. It will be described in detail in the following sections.

D. Chemical Propulsion System Architecture

In this chapter the architecture overview of the whole bipropellant subsystem will be given and technical decisions derived from the system requirements will be justified. The Chemical propulsion subsystem was developed to fulfill specific system requirements, stated in Table VII, and assumptions depicted in the Table ?? and it is unique technical solution. The flow chart of the chemical subsystem with all the relevant details is shown in Figure 17 in the Appendix A. From the mission design it is derived that the first five maneuvers are performed using chemical propulsion including MOI which is the most demanding one concerning the overall propulsion subsystem. The main engine S400-15 from ArianeGroup shall provide the necessary thrust for this orbit insertion maneuver, the trajectory correction maneuver and remaining maneuvers while twelve ArianeGroup RCS thrusters S10-26 shall provide the thrust for a 3-axis attitude control once arrived in orbit around Phobos for at least two years. These two off the shelf bipropellant thrusters meet the requirements of this mission

and are chosen also considering economic reasons and heritage of around 40 completed missions for the S400-12 and S400-15 engines. Both selected thrusters are helium pressurized and use monomethyl-hydrazine (MMH) as fuel and mixed oxides of nitrogen MON-3 as oxidizer. From the flow chart it is visible that two 40 liter tanks are used for pressurized helium. To fill the tanks and access the fluid, fill and drain valves are placed after every tank. Helium is leaving the pressurant tanks with 310 bar and goes through a dual mechanical pressure regulator which lowers the pressure to 20 bar. Normally closed pyro valves are placed before and after pressure was regulated to isolate it in case of any leakage. Redundant check valves are ensuring that the flow is going only in the direction of the propellant tanks and safety relief valves are placed in case of any kind of over pressurisation of helium before entering the pressurization tanks. To secure that propellants are not going upstream and mixing with helium, normally closed pyro valves are placed before the propellant tanks. In the feed line of the main engine, pyro ladders are introduced and are chosen due to their redundancy and minimum leakage. Furthermore, the mission is designed in a way that the main engine is passivated in between the second and third maneuver due to long waiting time as well as after fifth (last chemical) maneuver which leads to a possible leakage of propellants. The pyro ladder will isolate main engine during these periods and ensures redundant access to the main engine. Upstream the RCS thrusters latch valve is placed to control the propellant flow for attitude control. The latch valves are used because of their ability to open and close numerous times which is advantageous in the case of attitude control. The S10-26 are dual seat thrusters meaning they have two flow control valves serially connected which allow a more precise attitude control and the shutdown of a thruster in case of a failure or malfunction.

E. Chemical Propulsion System Mass Budget

To compute the dry mass of the chemical subsystem, the component selection is iterated throughout the development process to ensure a failure free mission by choosing off the shelf equipment while taking into account heritage from already completed missions. The current baseline consists of the equipment listed in the Table X. One of the assumptions of this mission is to have an all European component design, but at this point of development some of the selected components are outside of Europe and are marked in orange. In future development steps, this should be replaced with European components to fulfill the CPROP.008 requirement and reduce cost. Taking into account the ESA margin philosophy [2], a margin of 20% is applied on pipes and 5% for off the shelf components.

TABLE X
BIPROPELLANT PART LIST

| Description | Type/Manufacturer | Amount | Mass per unit [kg] | Margin | Mass inc. margin |
|-------------------------|-------------------|--------|--------------------|--------|------------------|
| Pipes | Pipes | 1 | 2.540 | 0.2 | 3.048 |
| Main Engine | S400-15 | 1 | 5.200 | 0.05 | 5.460 |
| RCS Thruster | S10-26 | 12 | 1.800 | 0.05 | 8.190 |
| Helium Tank | PVG Family 40l | 2 | 8.500 | 0.05 | 18.700 |
| Fuel Tank | OST 25/0 | 1 | 21.000 | 0.05 | 22.050 |
| Oxide Tank | OST 25/0 | 2 | 21.000 | 0.05 | 44.100 |
| Fill Vent Valve | ArianeGroup | 3 | 0.060 | 0.05 | 0.315 |
| Latch Valve | ArianeGroup | 4 | 0.545 | 0.05 | 2.289 |
| Pyro Isolation Valve | ArianeGroup | 16 | 0.160 | 0.05 | 2.688 |
| Safety Relief Valve | Safran | 2 | 0.700 | 0.05 | 1.470 |
| Check Valve | Vacco | 4 | 0.020 | 0.05 | 0.084 |
| Filter | Vacco | 8 | 1.500 | 0.05 | 12.600 |
| Dual Pressure Regulator | Stanford Mu | 1 | 1.130 | 0.05 | 1.187 |
| Pressure Transducer | Bradford Space | 5 | 0.230 | 0.05 | 1.207 |
| Thermocouples | Collins Aerospace | 12 | 0.350 | 0.05 | 4.410 |
| Total | | | | | 126.948 |

F. Chemical Propellant Budget

TABLE XI
CHEMICAL PROPELLANT BUDGET

| | [kg] | [kg] |
|-----------------|----------------|----------------|
| Maneuver Name | MMH | MMO |
| C3 | 116.714 | 192.578 |
| TCM | 0.290 | 0.478 |
| MOI | 155.285 | 256.221 |
| Match INC | 2.298 | 3.791 |
| Raise Peri min | 0.169 | 0.280 |
| Total Chemical | 274.756 | 453.348 |
| Margin 1% AOGNC | 2.748 | 4.533 |
| Margin 2% | 5.495 | 9.067 |
| Margin Sum | 8.243 | 13.600 |
| Leftover | 8.744 | 14.427 |
| Total | 283.500 | 467.775 |

G. Helium Fill Level, Pressure and Temperature in Pressurant and Propellant Tanks

The feeding system for the propellant tanks is pressure regulated to enable for consistent and predictable performance and to optimize fuel efficiency, which is important for a long-duration mission. A pressure regulated system requires the pressurant gas to be stored in additional tanks. In the presented bipropellant system, the propellant tanks are pressurized with Helium stored in two 40-liter tanks from MT Aerospace [9].

The options considered as a pressurant gas were helium and nitrogen, which were determined by the selected propellant tanks. Helium is used as a pressurant gas due to the following advantages over nitrogen:

- its lower density, which means it can provide the same pressure at lower mass or volume
- a lower viscosity, useful for precise flow control and better flow over small orifices and valves

- it is non-reactive even at high temperatures and pressures, making it ideal for use in a pressurized system where contamination or chemical reactions can be a concern

However, there are also some disadvantages to using helium over nitrogen. For example, helium is more expensive and less widely available than nitrogen, which can make it less cost-effective. Nonetheless, its low density and thus reduction of the launch mass is the deciding factor in favour of helium.

To guarantee the required operation of the bipropellant chemical thrusters, thereby contributing to requirement CPROP.001, a thorough analysis of the Helium fluidic conditions throughout the bipropellant engine operation is performed. This analysis is based on the assumptions listed on Table XII.

TABLE XII
ASSUMPTIONS PRESSURANT TANK SIZING

| Assumptions | |
|-------------|--|
| 1 | The initial ullage volume in the propellant tanks is filled with Helium before the start of operation. |
| 2 | The temperature of Helium in the propellant tanks is calculated as the equilibrium temperature between the Helium in the tank and the incoming Helium from the pressure regulator. |
| 3 | The temperature increase of Helium over the pressure regulator due to the Joule-Thomson effect is averaged over the maneuver time with the conditions at the beginning and end of the maneuver. |
| 4 | Heat transfer in Helium within the propellant tanks at the liquid-vapour interface and at the tank walls is neglected. |
| 5 | The required combustion chamber inlet pressure is 18.5 bars and the pressure drop between the propellant tanks and the thruster is 1.5 bars, leading to a required propellant tank pressure of 20 bars |

For the propulsion system design, one of the most relevant parameters is the amount of helium required in the system since it influences the launch mass, both directly as additional wet mass and indirectly as it affects dry mass of the required pressurant tanks. In order to maintain the required engine operation, the pressurization system shall contain enough helium for all foreseen maneuvers and at least an additional ullage mass of 20 %. Table XIII shows the fulfillment of these conditions.

TABLE XIII
PRESSURANT TANK MARGIN

| | |
|---|---------------|
| Initial Helium Mass in Pressurant Tank [kg] | 3.266 |
| Total Helium Mass maneuvers [kg] | 1.961 |
| Leftover Helium in pressurant tank [kg] | 1.305 |
| Pressurant Mass Margin [%] | 40.000 |
| Required Pressurant Mass Margin [%] | 20.000 |

Regarding the selection of the pressurant tanks, two suppliers were considered: Northrop Grumman and MT Aerospace. Despite the higher range of volumes offered by the Northrop Grumman [10], it was not selected because of its US origin (CPROP.008). The high-pressure helium tanks offered by MT aerospace have a Mean Operating Pressure (MEOP) of 310 bars, which results in a total volume of helium of 48 liters required for maneuvers. Considering an ullage volume of

20 %, the volume of helium shall be at 57.6 (m^3) [4]. Nevertheless, the sizing of the helium tanks is not only dependent on the required volume, but also on the helium pressure and temperature conditions, both in the propellant and in the helium tanks. For this reason, a fluidic simulation was performed with the following objectives:

- guaranteeing safe propellant conditions;
- maintaining the pressure of helium within the pressurant tanks above the 20 bars required in the propellant tanks;
- keeping the helium temperature within the pressurant tank between - 30 and + 60°C as specified by the tank supplier (Table XXVII);

The calculated pressure and temperature conditions of helium within the pressurant tanks throughout the maneuvering time are depicted in figures 8 and 7. For this calculation, only the first five maneuvers are considered, since the remaining maneuvers are not performed with the chemical engine. As observed in figure 7, the helium pressure is still above 100 bars after the last chemical maneuver, leaving more than enough margin for the RCS thruster operation. The temperature of helium within the pressurant tank remains between - 20 and + 50°C, as depicted in figure 7 fulfilling the aforementioned tank temperature constraint. In order to keep the temperature in this range, a heater is added to the pressurant tank. This heater is active in between maneuvers, as well as during the biggest maneuvers, which coincide with the biggest pressure and temperature drops in the charts: the first and third maneuver, namely C3 and MOI respectively.

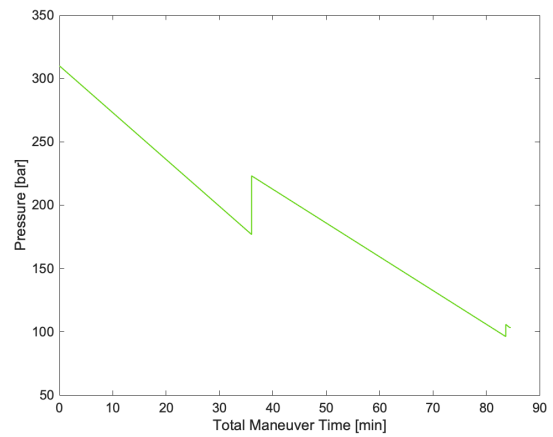


Fig. 7. Helium Pressure in Pressurant Tanks

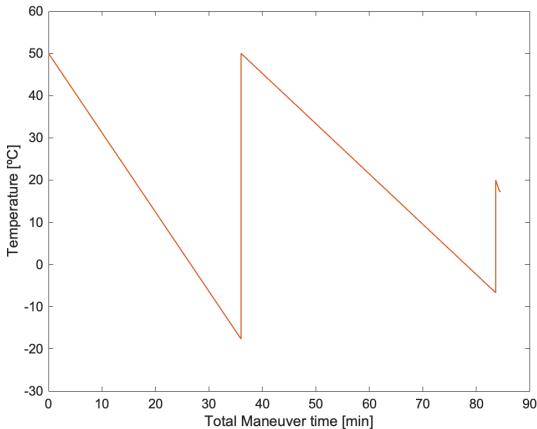


Fig. 8. Helium Temperature in Pressurant Tanks

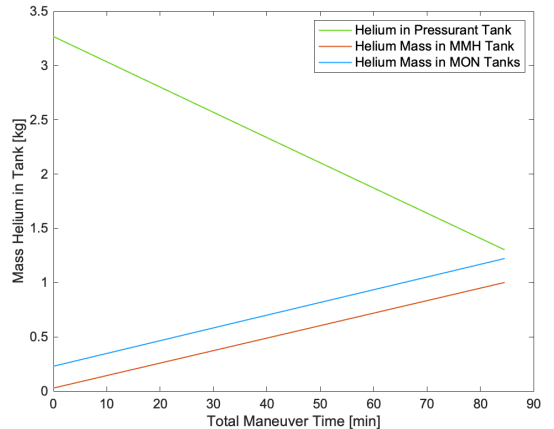


Fig. 9. Helium Mass in Tanks

Table XIV displays the exact pressure and temperature values at the beginning and end of each chemical maneuver, as well as the heating power required. The pressurant tank is warmed up to 50 °C before the beginning of operation and between the second and third maneuvers; and to 20 °C before the last two chemical maneuvers. The maximum heater power required is 200 W during the MOI maneuver, which can be easily provided by the power system since at this point of operation, the electric engine is still not in use.

TABLE XIV
PRESSURANT TANK SIZING

| | [m/s] | [kg] | [bar] | [°C] | [W] | | | |
|---|---------|-----------------|--------------------|--------------------|--------|--|--|--|
| Maneuver Name | Delta v | Helium required | Pressure | Temperature | Heater | | | |
| C3 | 509.350 | 0.836 | 310.000 177.175 | 50.000 -17.479 | 50 | | | |
| TCM | 34.553 | 0.002 | 177.175 176.903 | -17.479 -17.635 | OFF | | | |
| Waiting time | | | 223.156 | 50.000 | ≤50 | | | |
| MOI | 751.782 | 1.105 | 223.156 96.268 | 50.000 -6.683 | 200 | | | |
| Waiting time | | | 105.854 | 20.000 | ≤50 | | | |
| Match INC | 13.153 | 0.017 | 105.854 103.498 | 20.000 17.369 | OFF | | | |
| Rais Peri min | 35.660 | 0.001 | 103.498 103.332 | 17.369 17.184 | OFF | | | |
| Total Helium Mass maneuvers [kg] | 1.961 | | | | | | | |
| Ullage Helium in propellant tanks [kg] | 0.259 | | | | | | | |
| Leftover Helium in pressurant tank [kg] | 1.305 | | | | | | | |
| Total Helium Mass [kg] | 3.525 | | | | | | | |

As shown in the last four rows of the table, the total amount of helium required in the system is 3.525 kg, accounting for the helium within the pressurant tanks and the initial helium within the propellant tanks filling their ullage volume. The mass distribution of helium within the bipropellant feeding system throughout the maneuvering time is depicted in Figure 9.

With respect to guaranteeing safe propellant operation, the relevant parameter is the helium temperature within the propellant tanks. It is critical to prevent the freezing of the propellants during operation. The freezing temperature of MMH is - 52 °C [11] and -15 °C for MON-3 [12] at a pressure of 20 bars. The upper temperature limit is defined by the boiling temperatures at this pressure condition, which are approximately 87 °C for MMH and 56 °C for MON-3 [13]. Figure 10 shows that the temperature of helium within the propellant tanks stays between 20 and 36 °C throughout operation, within the propellants' safe temperature range.

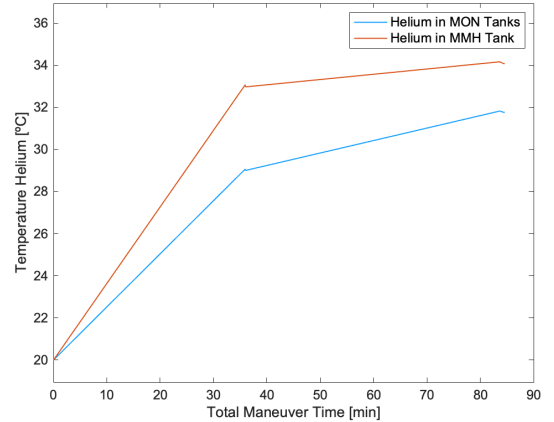


Fig. 10. Helium Temperature in Propellant Tanks

H. Reaction Control System (RCS)

The RCS system is based on the CPROP.002 requirement, shown in Table VII. To design this RCS system, an allowable engine offset and misalignment is needed. In this case, the engine offset can be interpreted as an offset of the center of gravity from the main axis as well. An allowable offset of 60 mm is given for the launch phase as a static unbalance for a three-axis stabilized spacecraft in the launchers user's manual [3]. For the design of this RCS system, a similar offset shall be chosen. In this case, the static offset shall not be traced back to the misplacement of the engine as the only source.

For the engine misalignment, the Ice Giants mission is used as a reference [7]. The resulting allowable combined engine errors are depicted in XV. Because the RCS system is not only needed for the compensation of the main engine moments in the thrust phases, but also for the AOGNC maneuvers, namely the desaturation of the reaction wheels while in the station keeping phase around Phobos, the RCS system shall be placed at the location where it's needed for the longest time duration. This then leads to a positioning in the center of gravity plane at the station keeping phase. For the positioning of the RCS thrusters, the configuration displayed in Figure 11 is selected. This configuration of 12 thrusters each, shows an overall good static and dynamic tracking error as well as a redundancy of two thrusters and is also portrayed as the best out of 14 different configurations [14]. More thrusters would increase the redundancy but also lead to a higher system mass and more complex system because the piping needs to be considered as well. Therefore, this configuration is chosen. In it, each bipropellant RCS-engine has a thrust of 10.25 N for the given pressure of the propellant, which also feeds the main bipropellant engine.

TABLE XV
ALLOWABLE ENGINE MISALIGNMENT

| Allowable combined engine errors | |
|----------------------------------|------|
| Maximum offset [mm] | 50.0 |
| Maximum misalignment [deg] | 1.0 |



Fig. 11. RCS Thruster Configuration

V. ELECTRICAL PROPULSION SYSTEM

A. Electrical Propulsion System Requirements

TABLE XVI
ELECTRIC PROPULSION SYSTEM REQUIREMENTS

| Electric Propulsion System Requirements | |
|---|--|
| Req. ID | Statement |
| EPROP.001 | The total mass of the electric subsystem shall be as low as possible. |
| EPROP.002 | The additional power demand shall be as low as possible. |
| EPROP.003 | The thruster shall have a burntime of under one year to achieve the required deltaV. |
| EPROP.004 | All parts shall be originated from european manufacturers. |
| EPROP.005 | The thruster shall be capable to perform orbital maintenance |
| EPROP.006 | All components within the electric propulsion system shall be TRL9. |

B. Electrical Propulsion System Trade-off's

The electrical propulsion system is completely build around its key component, its thruster. In the thruster selection its specified thrust, power demand and specific impulse all together ultimately have driven the selection. Following EPROP.001, the lowest total mass is the target value to optimise for. The complete mass of the electrical propulsion system contains not only hardware and fuel mass but also the mass associated to meet the additional power demands. In compliance with EPROP.004 all to us available european electric thrusters have been collected and are evaluated in Table XXIX. To ensure EPROP.005, a minimal thrust of approximately 5 mN is required (discarded marked red). Using the impulsive delta v values by an uncertainty factor of 2, for the sections planned to be performed electrically, burn times can be computed. In order to set a limit in flight time and feature realistic operational times, EPROP.003 was created and applied. This additional requirement narrowed down the options significantly (discarded marked red). As EPROP.003 being an indirect requirement on thrust at roughly 80 mN, EPROP.005 is passively contained. From there, the fuel mass was calculated over delta v and specific impulse as well as the additional solar mass was derived from the linear part of the power mass Equation 4. The minimal sum of which leaded to the selection of the Safran PPS 1350 Hall Effect Thruster, which was additionally refined by trying out all narrowed down options in the mass_design.m script and comparing its launch masses. Both approaches concluded the same choice.

C. Electrical Propulsion System Architecture

To complete the system architecture, additional components have been selected suiting the Safran PPS 1350 Thruster. As suggested in the Safran Portfolio [15], the complete propulsion system for the SMART-1 lunar probe was presented as setup for this thruster. Conveniently almost all of the components can be transferred to this mission which lead to the copy of the system architecture of SMART-1 for this mission. Only the xenon tank did not suit the required fuel mass and had to be replaced as shown in Table XVII. This was additionally convenient since the xenon tank was the only part being manufactured outside of Europe and by this change EPROP.004 can remain fulfilled. Since only the subsystem drymass of SMART-1 was reported, the tank mass of the Lincoln Composites xenon Tank was estimated and deducted from the SMART-1 subsystem drymass. The adapted flowchart of the electrical propulsion system and connection of components can be seen in Figure 18 and the hardware in Figure 19.

D. Electrical Propulsion System Mass Budget

TABLE XVII
ELECTRIC PARTLIST

| Description | Manufacturer | Qt. | [kg] Mass per Unit | [kg] Marg. | [kg] Total Mass |
|--|------------------------|-----|-----------------------|---------------|--------------------|
| Hall Effect Thruster PPS 1350 | Safran (France) | 1 | | | |
| xenon Flow Controller | Safran (France) | 2 | | | |
| Bang-Bang Pressure Regulation Unit | Safran (France) | 1 | | | |
| xenon Tank 49 liter | Lincoln Comp. (USA) | 1 | > 5.000 | | |
| Power Processing Unit Thruster Switch Unit | ETCA (Belgium) | 1 | | | |
| Pressure Regulation Electronic Card | Atermes (France) | 1 | | | |
| SMART-1 subsys. drymass | | 1 | 29.000 | | |
| SMART-1 subsys. drymass without Xe tank | | 1 | 24.000 | 0.05 | 25.200 |
| xenon Tank S-XTA / 120l | MT Aerospace (Germany) | 1 | 16.800 | 0.20 | 20.160 |
| Total | | | | | 45.360 |

E. Power Budget and Solar Panel Sizing

Due to a very high efficiency of the Power Supply Unit (PPU), the total power demand of the electrical system is set equal to the power usage of the Hall Effect Thruster itself. Therefore, the power demand of the electrical system of 1500W is added to the base power usage of 550W which together is converted via the provided power system mass formula directly as seen in Equation 4 below. To transfer power requirements from Mars to Earth, the inverse-square law is used as in Equation 3. The additional power demand of the electric propulsion is consequentially scaling the power mass linearly by a factor of $0.0758 \cdot 1.524^2$ kg per Watt. The power system mass m_{PWR} (Equation 4) is including the mass of the solar arrays as well as the power conditioning hardware.

$$P_{\text{Earth}} = P_{\text{Mars}} \cdot 1.524^2 = 2050W \cdot 1.524^2 = 4761.3W \quad (3)$$

$$m_{\text{PWR}} = 0.0758 \frac{\text{kg}}{\text{W}} \cdot P_{\text{Earth}} + 37.741\text{kg} = 398.65\text{kg} \quad (4)$$

The surface area of the solar panels is directly derived by the solar constant at Mars E_{Mars} and an assumed solar cell efficiency of $\eta = 0.29$.

$$A_{\text{Solar}} = \frac{P_{\text{Mars}}}{\eta \cdot E_{\text{Mars}}} = \frac{2050W}{0.29 \cdot \frac{1361}{1.524^2} \frac{\text{W}}{\text{m}^2}} = 12.06\text{m}^2 \quad (5)$$

In order to fit a modular size for the solar panels, the solar array area is rounded up to $A_{\text{Solar}} = 13\text{m}^2$ into two symmetrical 6.5 m x 1 m sections.

F. Electrical Propellant Budget

TABLE XVIII
ELECTRICAL PROPELLANT BUDGET

| Maneuver Name | [kg] |
|---------------------|----------------|
| Circularize | 51.805 |
| Spiral Down Match | 56.065 |
| Orbital Maintenance | 6.982 |
| EOL | 47.725 |
| Total Electric | 162.578 |
| Margin 2% | 3.252 |
| Leftover | 3.422 |
| Total | 166.000 |

G. Technology Needs

Besides all other components being flight proven and align with EPROP.006, the selected xenon Tank from the S-XTA family of MT Aerospace is still under development and is therefore a technological need.

VI. SPACECRAFT ARCHITECTURE

A. Spacecraft Orientation

The orientation of the spacecraft in the quasi-satellite orbit around Phobos in respect to Phobos is chosen in a way, that the instruments always face Phobos, as displayed in Figure 12. To achieve such an orientation in the main axis frame of the spacecraft, a constant rotation around the Z-axis is needed. The rotation speed has to match one orbital period around Mars. In this case, a rotational period of 27576.2 seconds is needed. In this orientation, the AOGNC system shall provide the required torques to counter the induced orbital perturbations. For station-keeping, the electrical engine is used. The RCS thrusters enable reaction wheel desaturation of the AOGNC system by locking the spacecraft in place. While the chemical and electrical thrusters are placed alongside the X-axis of the spacecraft, the solar arrays are located alongside to Y-axis, where they can rotate freely around the axis without changing the spacecrafts attitude. This orientation is chosen to ensure sun-tracking of the solar arrays. As presented in Figure 13, the instrument and communication subsystem are located on the Z-axis to ensure, that the field of view is always in the direction of Phobos and undisturbed by the other parts of the spacecraft. In case of the transmission of data to Earth or the Mars Relay Network via i.e. NASA's Mars Reconnaissance Orbiter (MRO) or the Mars Atmospheric and Volatile EvolutioN (MAVEN) orbiter, the spacecraft can interrupt its constant rotation around the Z-axis to then point itself in the dedicated direction [16]. This capability is also needed for the orbital station-keeping maneuvers to point the X-axis, and therefore the thrust vector, respectively.

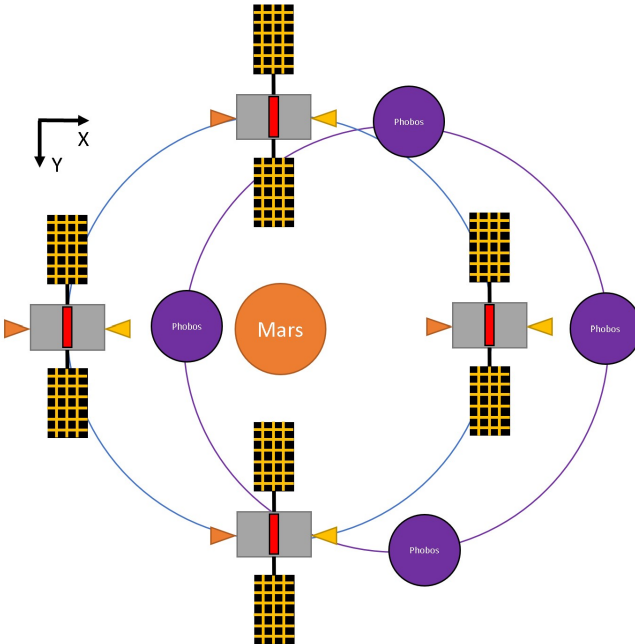


Fig. 12. Spacecraft orientation in XY-plane

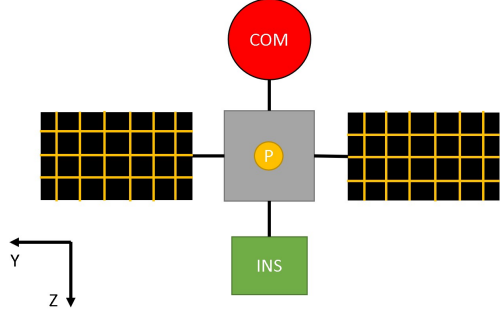


Fig. 13. Spacecraft orientation in YZ-plane

B. Spacecraft Stability Analysis

To ensure that a flat spin is not occurring during the mission phase around Phobos where a constant rotational speed is present, the following relation for the moments of inertia in the main axis system, shown in Equation 6, needs to be fulfilled [1].

$$I_z \geq I_y \geq I_x \quad (6)$$

While the components of the spacecraft that account for the dry mass, except the Phobos surface probe, are stationary in respect to the internal spacecraft frame, the propellants are not. Therefore the center of gravity (CoG) shifts over the mission as displayed in Table XIX. Since the CoG is the reference point for the calculation of the moments of inertia, these change as well over the duration of the mission, presented in Table XX. In all instances, the criteria set in Equation 6 is fulfilled. To further validate this stability analysis, the CoG can be

moved away from the X-axis by 60 mm in the Y- and Z-direction, which is the maximum tolerable limit given by the Ariane 6 user's manual for the static unbalance of a three-axis stabilized spacecraft [3]. With this offset, the moments of inertia, displayed in Table XXI result. In this case, the stability criteria is still valid, therefore the chosen configuration is feasible.

TABLE XIX
CENTER OF GRAVITY

| Center of gravity over time | | | | | |
|-----------------------------|--------|--------|--------|--------|--------|
| Point in time | 1 | 2 | 3 | 4 | 5 |
| CoG_x [m] | 1.6966 | 1.7322 | 1.7324 | 1.9146 | 1.9192 |
| CoG_y [m] | 0.0000 | 0.0000 | 0.0000 | 0.0000 | 0.0000 |
| CoG_z [m] | 0.0000 | 0.0000 | 0.0000 | 0.0000 | 0.0000 |
| Point in time | 6 | 7 | 8 | 9 | 10 |
| CoG_x [m] | 1.9196 | 1.8928 | 1.8613 | 1.8571 | 1.8276 |
| CoG_y [m] | 0.0000 | 0.0000 | 0.0000 | 0.0000 | 0.0000 |
| CoG_z [m] | 0.0000 | 0.0000 | 0.0000 | 0.0000 | 0.0000 |

TABLE XX
MOMENTS OF INERTIA

| Moment of inertia over time | | | | | |
|-----------------------------|--------|--------|--------|--------|--------|
| Point in time | 1 | 2 | 3 | 4 | 5 |
| I_x [kgm^2] | 3008.1 | 2885.0 | 2884.7 | 2720.8 | 2718.3 |
| I_y [kgm^2] | 5626.6 | 5571.0 | 5570.8 | 5496.9 | 5495.8 |
| I_z [kgm^2] | 7416.7 | 7238.0 | 7237.6 | 6999.8 | 6996.1 |
| Point in time | 6 | 7 | 8 | 9 | 10 |
| I_x [kgm^2] | 2718.1 | 2718.1 | 2718.1 | 2718.1 | 2718.1 |
| I_y [kgm^2] | 5495.7 | 5455.0 | 5411.0 | 5405.5 | 5368.1 |
| I_z [kgm^2] | 6995.8 | 6955.2 | 6911.2 | 6905.7 | 6868.3 |

TABLE XXI
MOMENTS OF INERTIA WITH AN OFF-CENTER COG BY 60 MM IN Y- AND Z-DIRECTION

| Moment of inertia over time | | | | | |
|-----------------------------|--------|--------|--------|--------|--------|
| Point in time | 1 | 2 | 3 | 4 | 5 |
| I_x [kgm^2] | 2967.7 | 2860.8 | 2860.5 | 2718.3 | 2716.0 |
| I_y [kgm^2] | 5631.4 | 5574.7 | 5574.6 | 5499.1 | 5498.0 |
| I_z [kgm^2] | 7372.4 | 7211.0 | 7210.6 | 6995.9 | 6992.6 |
| Point in time | 6 | 7 | 8 | 9 | 10 |
| I_x [kgm^2] | 2715.9 | 2715.5 | 2715.1 | 2715.1 | 2714.7 |
| I_y [kgm^2] | 5497.9 | 5457.1 | 5412.9 | 5407.3 | 5369.7 |
| I_z [kgm^2] | 6992.3 | 6951.5 | 6907.3 | 6901.8 | 6864.2 |

C. Spacecraft Launcher Compatibility

In this section it shall be analyzed, if the spacecraft complies with the requirements of the Ariane 62 launch vehicle, depicted in Table XXII. Here, the CoG envelope is a result from the given equations with the inserted spacecraft wet mass, which is presented in Table V for a spacecraft with a wet mass bellow 4 tons. By comparing these values with the spacecrafts characteristics in Table XXIII it can be demonstrated, that the requirements of the launch vehicle are fulfilled, even with a margin of 10 %. Also the moments of inertia in the transverse and rolling directing are within the given boundaries. Consequently, the spacecraft is suited for a launch with the Ariane 62 launch vehicle.

TABLE XXII
ARIANE 62 LAUNCH VEHICLE REQUIREMENTS [3]

| Ariane 62 launch requirements | |
|--|---------------------|
| Launch weight requirement [kg] | <2600.0 |
| Diameter [m] | <4.600 |
| CoG requirement in X [m] | 0.4887 <CoG <2.3663 |
| CoG requirement in Y and Z [m] | CoG <0.060 |
| Spacecraft transverse inertia momentum [kgm^2] | <90000 |
| Spacecraft roll inertia momentum [kgm^2] | <45000 |

TABLE XXIII
SPACECRAFT LAUNCH PARAMETERS

| Spacecraft launch parameters | |
|---|------------------|
| Launch weight [kg] | 2141.4 |
| Launch weight with 10 % margin[kg] | 2355.5 |
| Dimensions in X [m] | 4.000 |
| Dimensions in Y and Z (without RCS) [m] | 2.7058 x 2.7058 |
| Dimensions in Y and Z (with RCS) [m] | 2.7058 x 3.8250 |
| CoG in X [m] | 1.6966 to 1.9196 |
| CoG in X with 10% margin [m] | 1.5269 to 2.1116 |
| CoG in Y and Z [m] | 0.000 |
| Spacecraft transverse inertia momentum in Y [kgm^2] | 3008.1 |
| Spacecraft transverse inertia momentum in Z [kgm^2] | 5626.6 |
| Spacecraft roll inertia momentum in X [kgm^2] | 7416.7 |

To conclude this section, the spacecraft is shown in the chosen fairing, namely the A62 short fairing, in Figure 14 with its solar panels folded. The dimensions of the fairing are taken from the Ariane 6 user's manual [3].

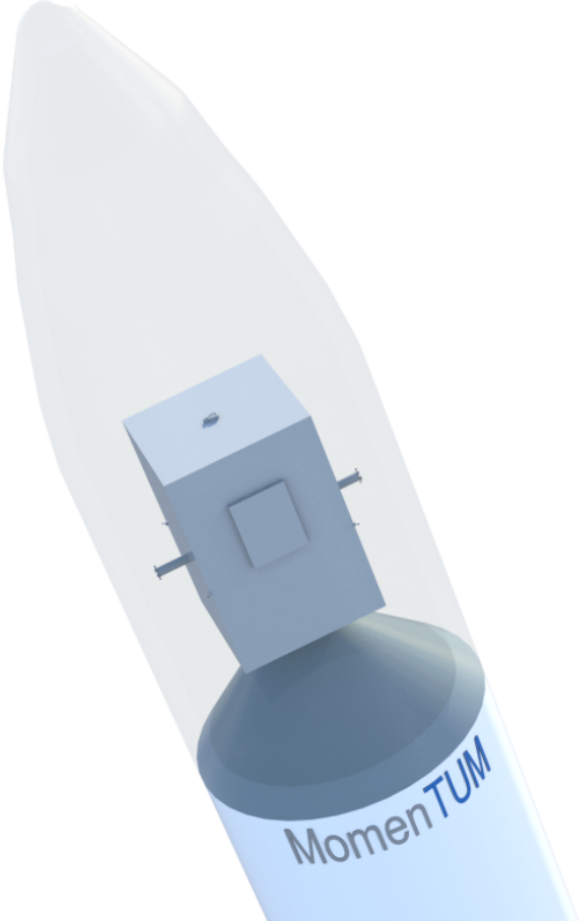


Fig. 14. Spacecraft in the A62 short fairing with undeployed solar arrays

D. Spacecraft Rendering

The final rendering of the spacecraft together with a rendering of the propulsion system of the spacecraft is visualized in this section. The first rendering shows the spacecraft in its orbital configuration with the solar arrays deployed in Figure 15. The key components that make up the chemical and electrical propulsion system together with the dedicated piping are shown in the second rendering, Figure 16. Special attention is given to the complex orientation of the pipes in 3D so that the amount of bends is equal between the respective MMH pipes from the tank in red and the MON-3 pipes form both tanks in light blue. This ensures a similar pressure drop over the pipes between the fuel tanks and the engine. The helium tanks in purple are located on top of the fuel tanks. In the middle right above the MMH tank is the xenon tank in cyan which feeds into the electrical propulsion system. More information about the placement of the individual parts is given in form of the technical drawings in the Appendix A.

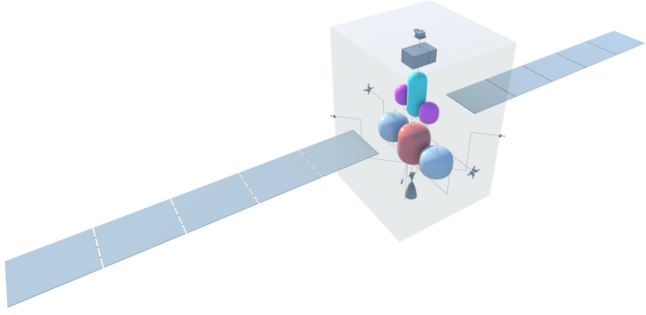


Fig. 15. Spacecraft with deployed solar arrays

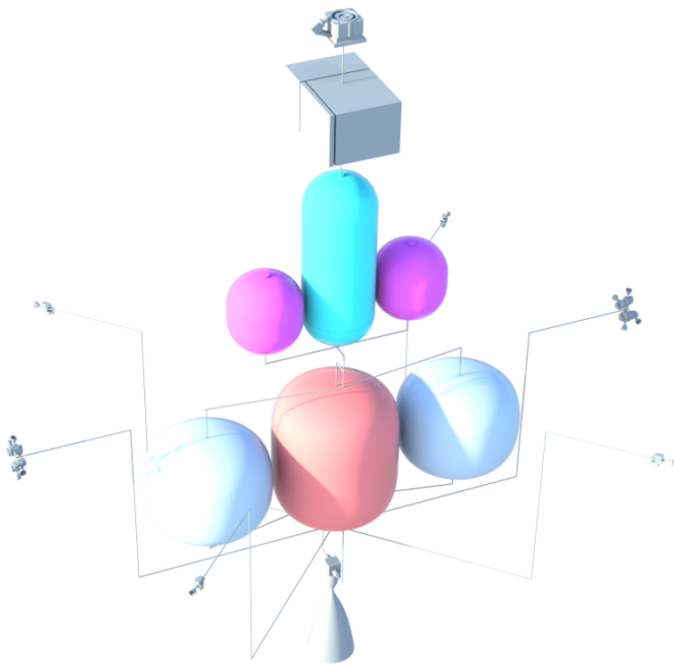


Fig. 16. Spacecraft Propulsion System

VII. SUMMARY AND LESSONS LEARNED

The report aimed to propose a preliminary design for the propulsion system of a spacecraft that will deliver a surface probe to Phobos. The concept presented combines a chemical and electrical engine, with all necessary components selected and displayed in their respective system schematics. The orbit trajectory selected to reach the destination with the proposed concept is also described. Simulations of the pressure and temperature of helium as a pressurant gas were performed and an analysis for the whole spacecraft stability and RCS thruster function was conducted, to ensure feasibility and safe operation.

The concept development process highlighted the complexity of designing a propulsion system for space missions. The main lesson learned by the team was that every component and aspect in the system is interconnected and that each design

decision has a significant impact on the overall system. For example, each small change in the mission trajectory affected the propellant budget which, affects the weight and feasibility of the propulsion system. Similarly, using two propellant tanks instead of one redefined many other aspects such as the launch mass, the pressurant gas calculation or the stability analysis.

The study presented a feasible preliminary design for the propulsion system, but there are still several open points that require further investigation. One such point is the design change of using one helium tank instead of two, which needs to be further analyzed for its feasibility and impact on the overall propulsion system. Furthermore, a more detailed calculation of the pressure drops over components and pipes needs to be conducted to redefine the pressure needed in the propellant tanks. This calculation could potentially affect the performance of the propulsion system. For the presented concept, the inlet pressure for the combustion chamber was taken as its maximum of 18.5 bars. However, its effect on the mixture ratio or efficiency of the engine, which requires further study. In case of the spacecraf's arrangement, the analysis is performed in a simplified manner. For a more detailed analysis, a CAD program can be used to analyze the behaviour of the center of gravity as well as the moments of inertia. Addressing these open points will improve the feasibility and performance of the proposed mission.

VIII. TEAM SETUP

A. Beatriz Mas Sanz - Systems Engineer

- 1) Project Plan and Requirements Definition
- 2) Propulsion System Trade-offs
- 3) Pressurant Tank Sizing Script

B. Marta Pelivan - Propulsion System Architect

- 1) Chemical Equipment Selection
- 2) Chemical Propulsion Architecture

C. Julian Schmid - Spacecraft System Architect

- 1) MATLAB script mass design
- 2) MATLAB script arrangement analysis
- 3) MATLAB script dV
- 4) 3D Assembly and technical drawings

D. Sven J. Steinert - Mission Analyst and IT Specialist

- 1) GMAT Trajectory and Evaluation
- 2) 3D Modelling
- 3) Electric Propulsion System

IX. ACCESS OF DATA

All presented files can be accessed in the Git-Repository.

X. INDIVIDUAL WORK - JULIAN SCHMID

A. Mass Budget Script and Validation

The mass budget script is a program written in MATLAB which is mainly used for the preliminary sizing of the spacecraft. Its main functions are the following:

- 1) Estimation of the dry, wet and launch mass as well as the PWR subsystem needs and mass, STR subsystem mass and the tank masses and volumes
- 2) Spacecraft mass behaviour over time
- 3) Calculation of the engine characteristics together with the calculation of the mixed ISP between the main engine and the RCS thrusters and the engine thrust as a function of the inlet pressure
- 4) Calculation of the main engine and RCS system propellant needs
- 5) Calculation of the needed solar array area

To make these calculations possible, the delta v's from the dV script as well as the already known subsystem masses and some key engine parameters have to be feed into the mass budget script. Two different approaches of calculating the spacecrafts wet mass are used and converged between each other to a residual of 10^{-3} , to calculate the spacecrafts mass. This is needed, because the spacecrafts STR subsystem is directly dependent on the wet mass of the spacecraft itself. In this process, the ESA margin philosophy [2] is respected. Different loop-starters are used to calculate a spacecraft wet mass in the first iteration by adding up all subsystem masses. After that, the resulting dry mass out of this calculation is fed forward to a step-wise calculation which utilizes the Tsiolkovsky rocket equation for each maneuver [1] to calculate a second wet mass. This wet mass is then compared to the wet mass in the additive approach before. If these values are too far apart, the values of the calculation that uses the rocket equation, namely the propellant mass, are fed back into the additive approach until the convergence is reached. In a later stage, the propellant mass can directly be inserted from GMAT. For the estimation of the propulsion system, namely the tank masses, a database of components is generated, which can be found in the Appendix A. This can then be compared to the mass, the tank would have if only Barlow's formula would be used [4]. In the script, Barlow's formula is used with the combined average over all deviating tank masses from the formula as a margin. This leaves the propulsion system with the engine and tank masses respectively. By then calculating the relation, the tanks and the engine account for the total propulsion system in an already proposed missions, a margin can be determined. This margin also includes the piping and other not considered propulsion elements. The Ice Giants mission form ESA [7] for a bipropellant or the Comet Interceptor mission from ESA [17] for an electric system can be used as a reference. To calculate the engine performance, a linear interpolation is made between the minimum and maximum point of engine thrust at the dedicated minimum and maximum inlet pressure of the main-engine (ME) and the

RCS thruster [8]. This is shown in Equation 7 for the S400-15 and Equation 8 for the S10-26 respectively in $\frac{N}{bar}$.

$$F_{S400-15} = \frac{450 - 340}{18.5 - 12.5} \cdot (p_{tank} - p_{loss}) + 110.833 \quad (7)$$

$$F_{S10-26} = \frac{12.5 - 6.0}{23.0 - 10.0} \cdot (p_{tank} - p_{loss}) + 1 \quad (8)$$

In terms of the main-engine efficiency, a mixed ISP is used between the main-engine and the RCS thrusters for the Tsiolkovsky rocket equation because two RCS thrusters have to compensate the shown engine misalignment and offset in Table XV. In this case, the maximum thrust of all engines is considered. Equation 9 shows this process.

$$ISP_{ME} = \frac{ISP_{ME} \cdot F_{ME} + 2 \cdot ISP_{RCS} \cdot F_{RCS}}{F_{ME} + 2 \cdot F_{RCS}} \quad (9)$$

In later mission planning phases, where multiple iterations between the mass budget and pressure drop script together with GMAT and the dV script occurred and a final flow-chart exists, the assumptions can be replaced by the chosen parts in the parts-list. For the PWR subsystem, the dedicated power requirements of each subsystem are inserted. By applying calculation logic, shown in the Section V-E, the mass of this subsystem can be calculated. By following these formulas, the solar array area is computed. To see if the assumptions in this mass budget script are valid, the Ice Giants mission from ESA is used as a validation reference for this tool. In Table XXIV it can be seen, that the discrepancy in the wet mass is low but not below 1 %. By tracing this error back it can be seen, that the biggest error lies in the propellant mass and not in the dry mass or the estimation of the propulsion system mass in general. One scenario where the divergence in the propellant mass can result from is, that the mass budget script does not accounting for the AOGNC maneuvers in the same way as the CDF report is. Since the mass budget script estimates a slightly higher wet mass, this error should be seen as an additional margin. For the estimation of the propulsion system mass as well as the dry mass, which is needed for the feedback into GMAT, this estimation is sufficient. Therefore, the mass budget script shall be used for the conceptual design process of this spacecraft.

TABLE XXIV
MASS BUDGET SCRIPT VALIDATION WITH ESA'S ICY GIANTS CDF REPORT [7]

| Mass Budget Script Validation | | |
|-------------------------------|------------|---------|
| | CDF Report | Script |
| Wet Mass [kg] | 4398.33 | 4540.60 |
| Wet Mass Error [%] | | 3.13 |
| Propellant Mass Error [%] | | 5.79 |
| Propulsion System Error [%] | | 0.74 |
| Dry Mass Error [%] | | 0.21 |

B. RCS Configuration Analysis

To decide, which RCS configuration shall be used for the mission, the following comparison is created based on the work in the following paper [14]. In this paper, 14 different configurations are created and analyzed in different categories. Because a configuration with less than 8 thrusters ensures no redundancy, only the configurations 6 to 14 are shown in Table XXV. By comparing the mean tracking error (MTE) in three axis as well as the level of redundancy (LR) it can be seen, that in configurations with 8 thrusters, only one thruster can fail to still ensure a three axis stabilized spacecraft. In systems with 16 thrusters, even 3 thrusters can fail. By calculating a ratio between the LR to the amount of thrusters it can be seen, that a system with 8 provides a ratio of 0.125, a system with 12 roughly 0.166 and a system with 14 a ratio of 0.1875. This shows, that a system with 16 is only slightly more redundant as a system with 12 compared to its amount of thrusters, while the static fuel consumption and the average pulses per thruster, for the reference case in the paper, are in the same range. Therefore, it is argued, that a system with 16 thrusters is not as beneficial as a system with 12 if the 16 thruster system has a similar MTE in three axis, as well as in total a higher fuel consumption and more mass. The piping is also more complex, leading to a higher system mass overall. By then comparing the RCS configurations with 12 thrusters individually it can be seen, that the best MTE and the least amount of pulses can be achieved with configuration 10, while having a similar fuel consumption as concepts 11 and 12. Consequently, configuration 10 is chosen for the spacecraft. By investigating the trade-off between a cold-gas nitrogen (N2) and a bipropellant RCS system with MMH and MON-3, as demonstrated in Table XXVI, it can be shown, that a system that uses bipropellant as its propellant is lighter in the chosen spacecraft configuration. The reference case for this trade-off is a mission, that only uses a bipropellant engine. This is not only due to the low ISP of the cold gas system but also since the main engine already uses bipropellant, a common feeding system can be utilized and therefore mass saved.

TABLE XXV
RCS CONFIGURATION ANALYSIS [14]

| RCS configuration trade-off | | | | |
|---------------------------------|---------------------------------|---|------------------------------------|--------|
| Config (number of thrusters) | Static Fuel Consumption [kg] | Mean Tracking Error Three Axis [deg] | Average Pulses per Thruster [1] | LR [1] |
| 6 (8) | 56.32 | 0.060 | 289 | 1 |
| 7 (8) | 50.54 | 0.057 | 178 | 1 |
| 8 (8) | 52.11 | 0.057 | 199 | 1 |
| 9 (8) | 79.40 | 0.220 | 309 | 1 |
| 10 (12) | 49.46 | 0.051 | 158 | 2 |
| 11 (12) | 50.81 | 0.077 | 221 | 2 |
| 12 (12) | 47.05 | 0.076 | 224 | 2 |
| 13 (16) | 46.49 | 0.047 | 174 | 3 |
| 14 (16) | 47.05 | 0.046 | 188 | 3 |

TABLE XXVI
RCS PROPELLANT TRADE-OFF [14]

| RCS Propellant Trade-off | | | |
|----------------------------------|--------|--------|--------|
| | N2 | N2 | Biprop |
| Storage Temperature [K] | 293.15 | 77.00 | 293.15 |
| RCS Engine Mass (8 engines) [kg] | 0.18 | 0.18 | 5.46 |
| RCS Propellant Mass [kg] | 282.02 | 189.00 | 93.66 |
| RCS Tank Mass [kg] | 190.02 | 33.45 | 0.45 |
| Total RCS System Mass [kg] | 472.22 | 222.63 | 99.57 |

C. Arrangement Analysis

In this section, the working principle of the arrangement analysis script (AAS) shall be described. The script itself is written in MATLAB and mainly used, to compute the center of gravity (CoG) and the moment of inertia (MoI) in the main axis frame of the spacecraft for each point in time. For that, a simplified model is set up. At first, the satellite shall be seen as a cuboid with a constant density distribution. All other parts with their known geometry, shape, location and mass are described as point-masses at a fixed location. This is demonstrated in Figure 23 in the XY-plane and Figure 24 in the Appendix A. To determine the location of the parts as well as the outer dimensions of the spacecraft itself, a feedback loop between the 3D-model and the AAS is used. The dry mass can then be split up into the known parts and into the rest, that is allocated to the cuboid. Because the spacecraft is loosing mass in form of propellant over each maneuver, the CoG is changing. To account for that, additional point masses are introduced, which represent the propellant. These masses start out in the center of their respective tank and move towards the bottom of the tank. While the total propellant mass and flow is taken from GMAT and the dV script, the flow of helium is a direct result of the pressure drop script. In this simulation, the movement of the CoG is limited to the X-direction. The result in the CoG shift is presented in Table XIX. With this information, the solar panels and the subsystems, INS and COM, as well as the RCS system, can be placed at the location of the CoG before the 8th maneuver. This location is chosen because it is assumed, that the RCS thrusters are mainly used in the quasi-satellite orbit phase for AOGNC maneuvers. The solar panel mass is determined with its area from the mass budget script and a conversion factor of 5.67kg/m^2 [18]. After this placement, the CoG has to be computed again. Since the solar panels are placed in the Y- and the INS and COM subsystem in the Z-direction, control over the systems MoI is possible. Therefore, it can be guaranteed, that the stability condition, presented in Equation 6 is satisfied. While the satellites cuboid uses the moment of inertia for a volumetric body, all other masses shall be taken into account with the parallel-axis theorem around the CoG [19]. The resulting MoI's are displayed in Table XX. Finally, a moment equilibrium around the CoG between the misaligned and offset main engine and the RCS system can be computed. The launcher requirements, shown in Table XXIII as well as the stability conditions and the disturbance torques need to be satisfied.

REFERENCES

- [1] U. Walter, *Astronautics: The Physics of Space Flight*. Springer eBook Collection, Cham: Springer International Publishing, 3rd ed. 2018 ed., 2018.
- [2] European Space Agency, “Margin philosophy for science assessment studies,” 2011. Available at https://sci.esa.int/documents/34375/36249/1567260131067-Margin_philosophy_for_science_assessment_studies_1.3.pdf Issue 1 Revision 3.
- [3] ArianeSpace, “ARIANE 6 USER’S MANUAL,” 2016. Available at https://www.arianespace.com/wp-content/uploads/2021/03/Mua-6-Issue-2_Revision-0_March-2021.pdf Issue 2 Revision 0.
- [4] C. Manfletti and S. Heizmann, “Spacecraft Propulsion and Design Challenge,” 2022. Available at <https://www.moodle.tum.de/course/view.php?id=80904>.
- [5] Laura M. Burke, Robert D. Falck, and Melissa L. McGuire, “Interplanetary mission design handbook: Earth-to-mars mission opportunities 2026 to 2045 - nasa technical reports server (ntrs),” 2010. Available at <https://ntrs.nasa.gov/citations/20100037210>.
- [6] H. Chen, E. Canalias, D. Hestroffer, and X. Hou, “Effective stability of quasi-satellite orbits in the spatial problem for phobos exploration,” *Journal of Guidance, Control, and Dynamics*, vol. 43, pp. 2309–2320, Dec. 2020.
- [7] European Space Agency, “CDF Study Report Ice Giants: A Mission to the Ice Giants – Neptune and Uranus,” 2019. Available at https://sci.esa.int/documents/34923/36148/1567260384517-Ice_Giants_CDF_study_report.pdf.
- [8] ArianeGroup, “10N, 200N, 400N CHEMICAL BI-PROPELLANT THRUSTER FAMILY: CHEMICAL BI-PROPELLANT THRUSTER FAMILY.” Available at https://satcatalog.s3.amazonaws.com/components/1007/SatCatalog_-_ArianeGroup_-_S400-15_Biprop_Thruster_-_Datasheet.pdf?lastmod=20210710070603.
- [9] M. Aerospace, “Mt-tankkatalog.pdf.” <https://www.mt-aerospace.de/files/mta/tankkatalog/MT-Tankkatalog.pdf>, 2023. (Accessed on 03/28/2023).
- [10] “Pressurant tanks data sheets - sorted by volume - northrop grumman.” <https://www.northropgrumman.com/space/pressurant-tanks-data-sheets-sorted-by-volume/>. (Accessed on 03/30/2023).
- [11] M. Wade, “Mon/mmh.” <http://www.astronautix.com/m/monmmh.html>, 1997. (Accessed on 03/30/2023).
- [12] A. Crawls, “Basics of space flight: Rocket propellants.” <https://web.archive.org/web/20130521134626/http://www.braeunig.us/space/propel.htm>, 2004. (Accessed on 03/30/2023).
- [13] H. W. Huu P. Trinh, Christopher Burnside, “Assessment of mon-25/mmh propellant system for deep-space engines.” <https://ntrs.nasa.gov/api/citations/20190033304/downloads/20190033304.pdf>, 2019. (Accessed on 03/30/2023).
- [14] M. Pasand, A. Hassani, and M. Ghorbani, “A study of spacecraft reaction thruster configurations for attitude control system,” *IEEE Aerospace and Electronic Systems Magazine*, vol. 32, no. 7, pp. 22–39, 2017. Available at 10.1109/MAES.2017.160104.
- [15] Safran, “Spacecraft propulsion subsystems.” Available at <https://www.safran-group.com/sites/default/files/2022-11/Safran%20Spacecraft%20Propulsion%20-%20Brochure%20-%20Portfolio.pdf>.
- [16] National Aeronautics and Space Administration, “The Mars Relay Network Connects Us to NASA’s Martian Explorers,” 2021-02-16 00:00:00 UTC. Available at <https://mars.nasa.gov/news/8861/the-mars-relay-network-connects-us-to-nasas-martian-explorers/>.
- [17] European Space Agency, “CDF Study Report Comet Interceptor: Assessment of Mission to Intercept a Long Period Comet or Interplanetary Object.” Available at https://sci.esa.int/documents/34923/36148/CometInterceptor_CDF_Study_Report.pdf.
- [18] Jet Propulsion Laboratory, “Solar Power and Energy Storage for Planetary Missions,” 2015. Available at https://www.lpi.usra.edu/opag/meetings/aug2015/presentations/day-2/11_beachamp.pdf.
- [19] D. Gross, W. Hauger, J. Schröder, W. A. Wall, and J. Bonet, *Engineering mechanics*. Berlin: Springer, 2nd edition ed., 2018.
- [20] C. Koppel, F. Marchandise, D. Estublier, and L. Jolivet, “The smart-1 electric propulsion subsystem in flight experience,” in *40th AIAA/ASME/SAE/ASEE Joint Propulsion Conference and Exhibit*, American Institute of Aeronautics and Astronautics, June 2004.

APPENDIX A ADDITIONAL RESOURCES

TABLE XXVII
PRESSURANT TANK [9]

| Supplier | MT Aerospace |
|-------------------|---|
| MEOP | 310 bar |
| Total Volume | 40-75 l |
| Temperature Range | -30/ +60 °C |
| Tank Dry Mass | 8.5 – 14.4 kg |
| Tank Diameter | 432 mm |
| Tank Length | 467 - 728 mm |
| Material | Ti-6Al-4V (Shell) Ti-3Al-2.5V (Tube) Epoxy-based CFRP / T800 (Overwrap) |

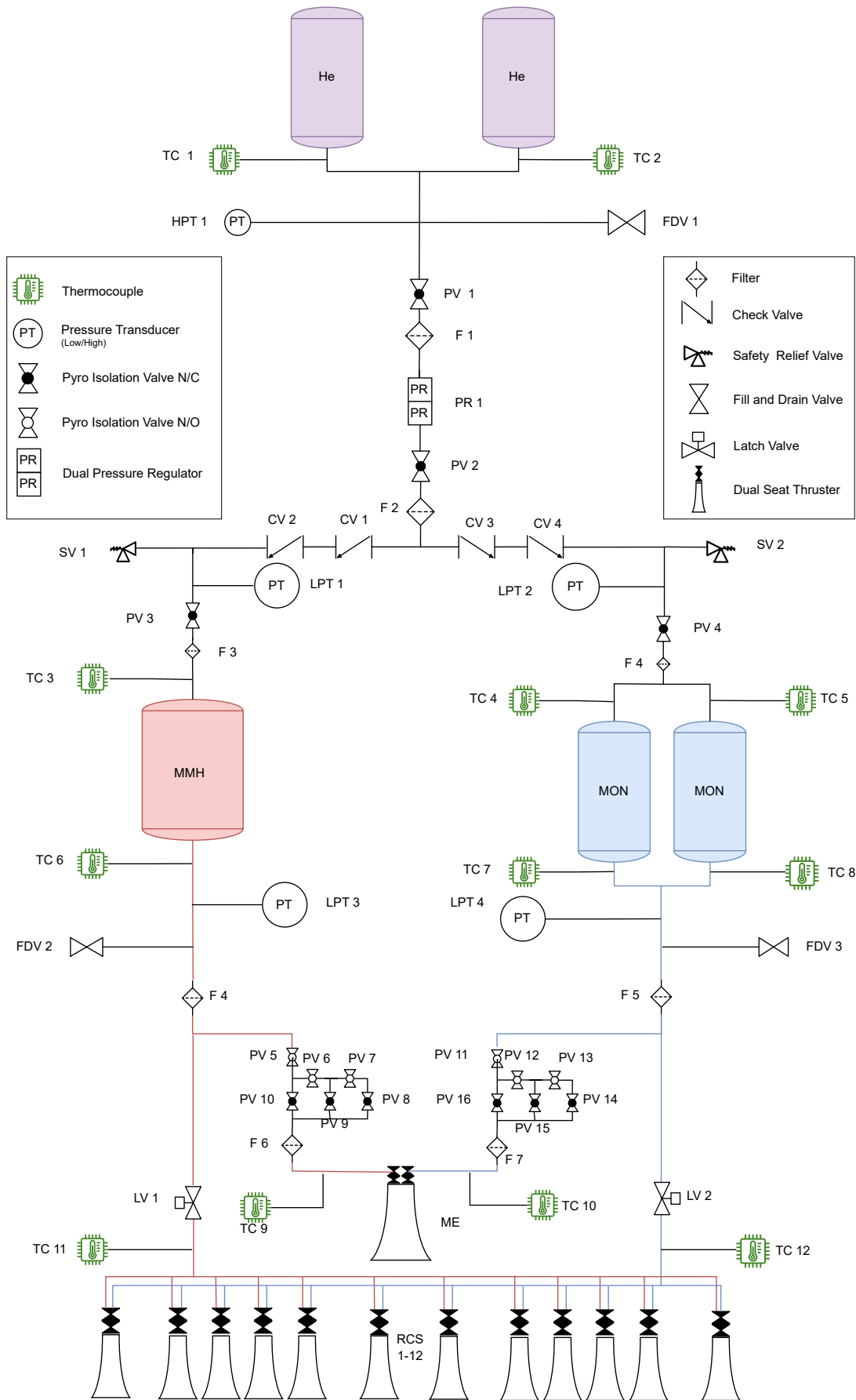


Fig. 17. Flowchart for Chemical Bipropellant Subsystem

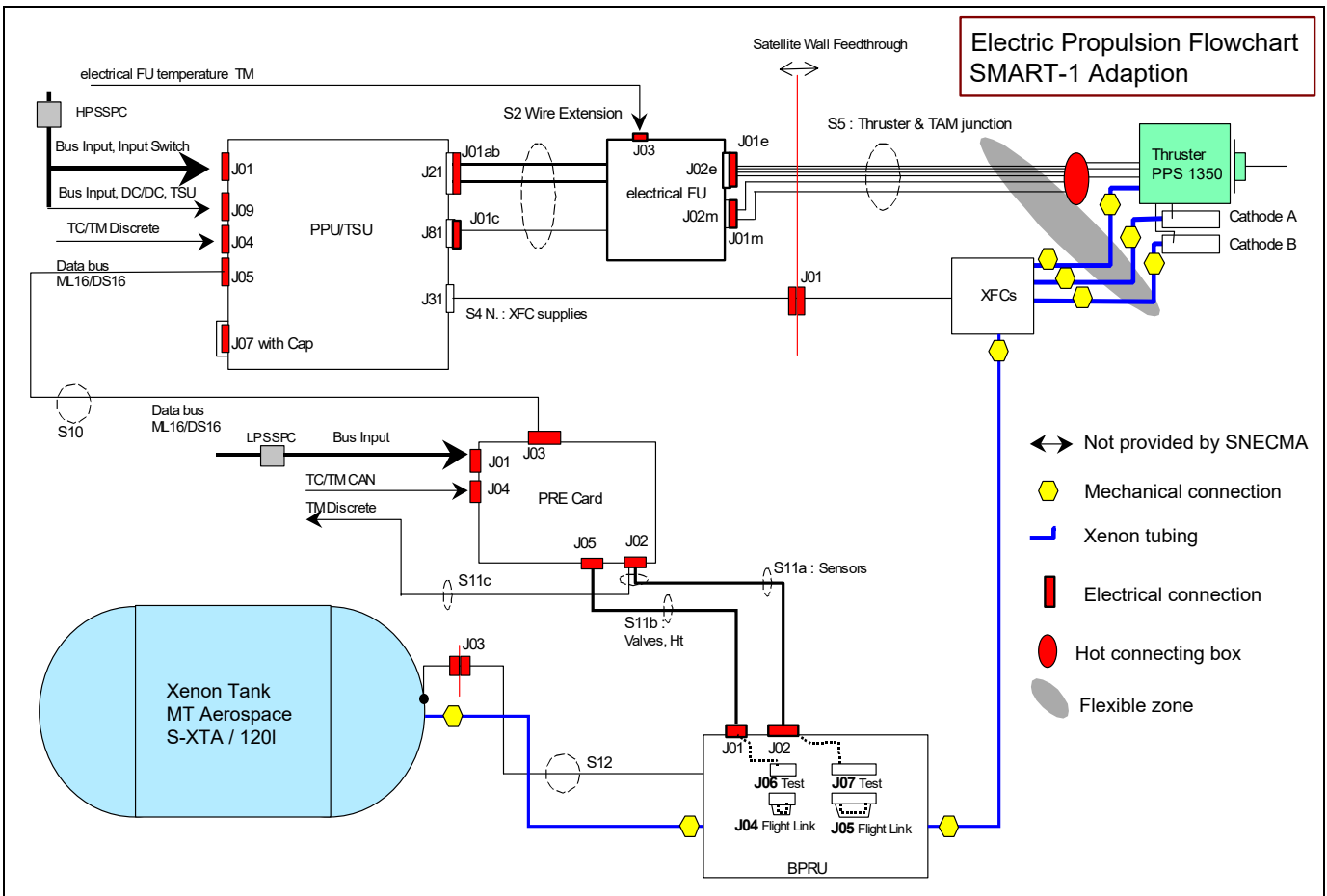


Fig. 18. Flowchart for Electrical Propulsion System as Adaption from SMART-1 [20]

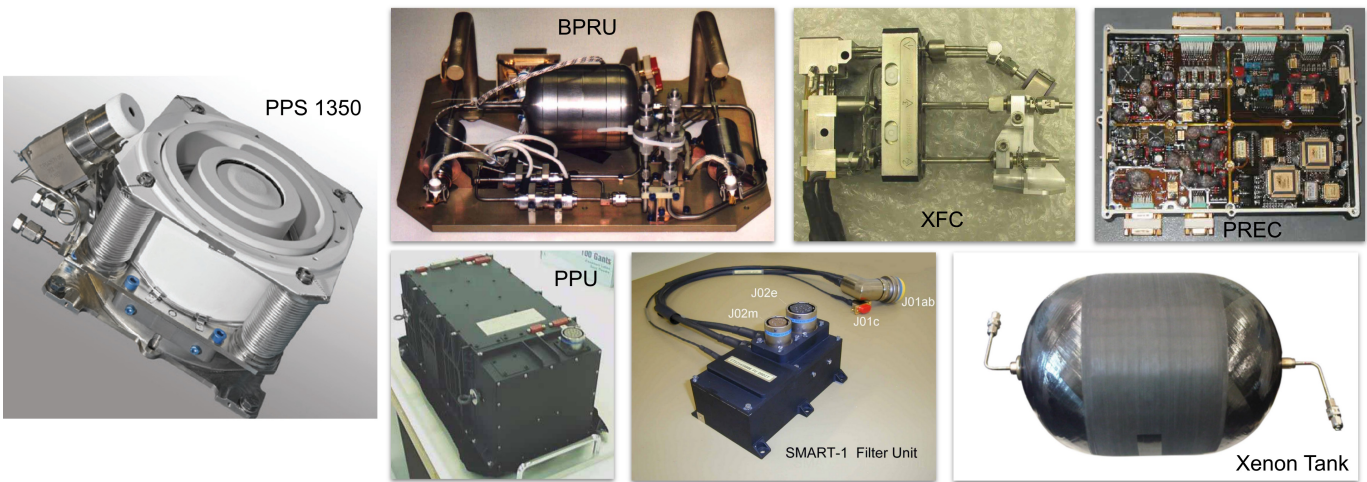


Fig. 19. Electric Propulsion Hardware adapted from SMART-1 [20]

TABLE XXVIII
MISSION TIMELINE

| Timestamp | | Maneuver Name | Drymass | [kg] | He | [kg] | MMH | [kg] | MMO | [kg] | Xe | [kg] | Total Mass |
|----------------------|-------|----------------------|----------------|-------|-----------|---------|------------|----------|------------|------|-----------|------|-------------------|
| 31 Oct 2026 12:00:00 | | Ariane 62 Mounted | 1226.589 | 3.525 | 283.500 | 467.775 | 166.000 | 2147.390 | | | | | |
| 31 Oct 2026 12:00:37 | | Ariane 62 Eject | 1141.589 | 3.525 | 283.500 | 467.775 | 166.000 | 2062.390 | | | | | |
| 03 Nov 2026 12:00:37 | Begin | C3 | 1141.589 | 3.525 | 283.500 | 467.775 | 166.000 | 2062.390 | | | | | |
| 03 Nov 2026 12:36:32 | End | C3 | 1141.589 | 3.525 | 166.786 | 275.197 | 166.000 | 1753.097 | | | | | |
| 21 Nov 2026 12:36:32 | Begin | TCM | 1141.589 | 3.525 | 166.786 | 275.197 | 166.000 | 1753.097 | | | | | |
| 21 Nov 2026 12:36:38 | End | TCM | 1141.589 | 3.525 | 166.496 | 274.719 | 166.000 | 1752.330 | | | | | |
| 17 Aug 2027 04:48:54 | Begin | MOI | 1141.589 | 3.525 | 166.496 | 274.719 | 166.000 | 1752.330 | | | | | |
| 17 Aug 2027 05:36:32 | End | MOI | 1141.589 | 3.525 | 11.752 | 19.392 | 166.000 | 1342.258 | | | | | |
| 28 Aug 2027 18:17:43 | Begin | Match INC | 1141.589 | 3.525 | 11.752 | 19.392 | 166.000 | 1342.258 | | | | | |
| 28 Aug 2027 18:18:25 | End | Match INC | 1141.589 | 3.525 | 9.455 | 15.600 | 166.000 | 1336.169 | | | | | |
| 29 Aug 2027 17:36:46 | Begin | Raise Peri min | 1141.589 | 3.525 | 9.455 | 15.600 | 166.000 | 1336.169 | | | | | |
| 29 Aug 2027 17:36:59 | End | Raise Peri min | 1141.589 | 3.525 | 8.744 | 14.427 | 166.000 | 1334.285 | | | | | |
| 22 Sep 2027 10:44:25 | Begin | Circularize | 1141.589 | 3.525 | 8.744 | 14.427 | 166.000 | 1334.285 | | | | | |
| 26 Aug 2029 16:26:15 | End | Circularize | 1141.589 | 3.525 | 8.744 | 14.427 | 114.195 | 1282.480 | | | | | |
| 27 Aug 2029 07:10:20 | Begin | Spiral Down Match | 1141.589 | 3.525 | 8.744 | 14.427 | 114.195 | 1282.480 | | | | | |
| 01 Jan 2030 14:43:40 | Begin | Wait Match | 1141.589 | 3.525 | 8.744 | 14.427 | 58.129 | 1226.414 | | | | | |
| 03 Jan 2030 00:29:49 | End | Wait Match | 1141.589 | 3.525 | 8.744 | 14.427 | 58.129 | 1226.414 | | | | | |
| 06 Jan 2030 21:28:19 | End | Spiral Down Match | 1141.589 | 3.525 | 8.744 | 14.427 | 56.458 | 1224.744 | | | | | |
| 06 Jan 2030 21:34:01 | | Arrived - Probe drop | 1121.589 | 3.525 | 8.744 | 14.427 | 56.458 | 1204.744 | | | | | |
| | | Orbital Maintenance | 1121.589 | 3.525 | 8.744 | 14.427 | 49.477 | 1197.762 | | | | | |
| 06 Jan 2032 21:34:01 | Begin | EOL | 1121.589 | 3.525 | 8.744 | 14.427 | 49.477 | 1197.762 | | | | | |
| 20 Apr 2032 12:31:53 | End | EOL | 1121.589 | 3.525 | 8.744 | 14.427 | 3.422 | 1151.708 | | | | | |

TABLE XXIX
ELECTRIC THRUSTER SELECTION

| Manufacturer | Name | Power [W] | Thrust [mN] | Isp [s] | Burntime [years] | Fuel Mass [kg] | Solar Mass [kg] | Sum Mass [kg] | Launch Mass [kg] |
|----------------|------------|--------------|----------------|------------|---------------------|-------------------|--------------------|------------------|---------------------|
| Morpheus Space | NanoFEEP | 0.2 | 0.001 | 3000 | 83443.5960 | 89.45 | 0.04 | 89.64 | |
| | | 3 | 0.02 | 8500 | 4314.1692 | 32.64 | 0.53 | 33.33 | |
| Morpheus Space | MultiFEEP | 0.4 | 0.001 | 7000 | 85944.8386 | 39.48 | 0.07 | 39.85 | |
| | | 1090 | 12.5 | 7000 | 6.8756 | 39.48 | 191.90 | 258.98 | |
| Rafael | R-200 | 140 | 4 | 800 | 18.1724 | 292.19 | 24.65 | 316.84 | |
| | | 350 | 14 | 1300 | 5.5770 | 193.14 | 61.62 | 254.76 | |
| Rafael | R-800 | 500 | 23 | 1300 | 3.3947 | 193.14 | 88.03 | 281.16 | |
| | | 1000 | 53 | 1550 | 1.5011 | 165.05 | 176.05 | 341.11 | |
| Safran | PPS X00 | 200 | 15 | 1300 | 5.2052 | 193.14 | 35.21 | 228.35 | |
| | | 1000 | 75 | 1650 | 1.0671 | 155.97 | 176.05 | 342.03 | |
| Safran | PPS 1350-G | 1500 | 90 | 1800 | 0.8961 | 144.08 | 264.08 | 437.16 | 1993.5841 |
| | | 2500 | 140 | 1800 | 0.5761 | 144.08 | 440.13 | 613.21 | 2487.5044 |
| Safran | PPS 1350-E | 2500 | 100 | 1600 | 0.7980 | 160.39 | 440.13 | 600.51 | 2547.0515 |
| | | 5000 | 300 | 1900 | 0.2700 | 137.11 | 880.26 | 1017.36 | 3685.1358 |
| Safran | PPS 5000 | 2500 | 150 | 1730 | 0.5358 | 149.40 | 440.13 | 615.53 | 2529.7035 |
| | | 5000 | 300 | 2000 | 0.2711 | 130.78 | 880.26 | 1043.03 | 3683.8819 |
| ArianeGroup | RIT uX | 50 | 0.5 | 3000 | 166.8872 | 89.45 | 8.80 | 98.25 | |
| ArianeGroup | RIT 10 EVO | 145 | 5 | 1900 | 16.2017 | 137.11 | 25.53 | 162.64 | |
| | | 435 | 15 | 3000 | 5.5629 | 89.45 | 76.58 | 166.03 | |
| | | 760 | 25 | 3200 | 3.3485 | 84.13 | 133.80 | 217.92 | |
| ArianeGroup | RIT 2X | 2000 | 70 | 3400 | 1.1993 | 79.40 | 352.10 | 431.50 | 2053.9215 |
| | | 2500 | 88 | 3500 | 0.9552 | 77.23 | 440.13 | 517.36 | 2273.0878 |
| | | 4000 | 151 | 3300 | 0.5552 | 81.70 | 704.21 | 785.90 | 2964.5545 |
| | | 4500 | 171 | 3500 | 0.4916 | 77.23 | 792.23 | 869.46 | 3172.3386 |
| | | 4800 | 198 | 2450 | 0.4166 | 108.27 | 845.05 | 953.32 | 3446.0344 |
| | | 5300 | 215 | 2750 | 0.3863 | 97.12 | 933.07 | 1030.19 | 3625.6223 |

TABLE XXX
TANK DATABASE

| Titanium Tanks (Monoprop / Biprop) | | | | |
|--|-----------------|----------------|---------------|---|
| Volume [l] | Ideal mass [kg] | Real mass [kg] | Margin-factor | Tank Source |
| 304 | 8.9643 | 17.5 | 1.95 | https://www.space-propulsion.com/spacecraft-propulsion/bipropellant-tanks/index.html#198 |
| 218 | 6.4284 | 11 | 1.71 | https://www.space-propulsion.com/spacecraft-propulsion/bipropellant-tanks/index.html#199 |
| 235 | 6.9297 | 16 | 2.31 | https://www.space-propulsion.com/spacecraft-propulsion/bipropellant-tanks/index.html#200 |
| 282 | 8.3156 | 21 | 2.53 | https://www.space-propulsion.com/spacecraft-propulsion/bipropellant-tanks/index.html#201 |
| 331 | 8.6514 | 22.7 | 2.62 | https://www.space-propulsion.com/spacecraft-propulsion/bipropellant-tanks/index.html#202 |
| 700 | 18.2959 | 36 | 1.97 | https://www.space-propulsion.com/spacecraft-propulsion/bipropellant-tanks/index.html#203 |
| 1108 | 28.9598 | 49 | 1.69 | https://www.space-propulsion.com/spacecraft-propulsion/bipropellant-tanks/index.html#204 |
| 769 | 18.0379 | 31.7 | 1.76 | https://www.space-propulsion.com/spacecraft-propulsion/bipropellant-tanks/index.html#205 |
| 1207 | 31.5474 | 52.5 | 1.66 | https://www.space-propulsion.com/spacecraft-propulsion/bipropellant-tanks/index.html#206 |
| 1309 | 34.2134 | 57 | 1.67 | https://www.space-propulsion.com/spacecraft-propulsion/bipropellant-tanks/index.html#207 |
| 1450 | 37.8987 | 61 | 1.61 | https://www.space-propulsion.com/spacecraft-propulsion/bipropellant-tanks/index.html#208 |
| 165 | 4.4232 | 10.8 | 2.44 | https://www.mt-aerospace.de/files/mta/tankkatalog/MT-Tankkatalog.pdf |
| | | | 1.993 | |
| CFRP-Titanium Tanks (Xenon) | | | | |
| Volume [l] | Ideal mass [kg] | Real mass [kg] | Margin-factor | Tank Source |
| 60 | 4.1329 | 11.7 | 2.83 | https://www.mt-aerospace.de/files/mta/tankkatalog/MT-Tankkatalog.pdf |
| 40 | 2.7553 | 6.3 | 2.29 | https://www.mt-aerospace.de/files/mta/tankkatalog/MT-Tankkatalog.pdf |
| 120 | 8.2658 | 14.8 | 1.79 | https://www.mt-aerospace.de/files/mta/tankkatalog/MT-Tankkatalog.pdf |
| 600 | 41.3288 | 68 | 1.65 | https://www.mt-aerospace.de/files/mta/tankkatalog/MT-Tankkatalog.pdf |
| 900 | 61.9932 | 85 | 1.37 | https://www.mt-aerospace.de/files/mta/tankkatalog/MT-Tankkatalog.pdf |
| | | | 1.985 | |
| CFRP-Titanium Tanks (Helium, Nitrogen) | | | | |
| Volume [l] | Ideal mass [kg] | Real mass [kg] | Margin-factor | Tank Source |
| 40 | 4.5675 | 8.5 | 1.86 | https://www.mt-aerospace.de/files/mta/tankkatalog/MT-Tankkatalog.pdf |
| 75 | 8.5641 | 14.4 | 1.68 | https://www.mt-aerospace.de/files/mta/tankkatalog/MT-Tankkatalog.pdf |
| 120 | 13.7026 | 23.5 | 1.72 | https://www.mt-aerospace.de/files/mta/tankkatalog/MT-Tankkatalog.pdf |
| | | | 1.752 | |

| | | Biprop only (US) | | Biprop only (EU) | | Biprop-Elec (US) | | Biprop-Elec (EU) | |
|----------------------|--|-----------------------------------|----------|------------------|----------|------------------|-----------|------------------|-----------------------------------|
| | | Evaluation | | Evaluation | | Evaluation | | Evaluation | |
| | | Value | | Value | | Value | | Value | |
| | | Weighting | | | | | | | |
| More imp than | | Propulsion System Wet Mass | 0 | 2 | 2 | 2 | 10 | 33,33% | Propulsion System Wet Mass |
| | | Volume propulsion system | 0 | 2 | 0 | 1 | 0 | 3 | 10,00% |
| | | Power Requirement | 0 | 0 | 0 | 1 | 1 | 2 | 6,67% |
| | | Industrialization | 0 | 2 | 2 | 2 | 8 | 26,67% | Industrialization |
| | | Technological risk | 0 | 1 | 1 | 0 | 2 | 4 | 13,33% |
| | | Propellant Toxicity | 0 | 2 | 1 | 0 | 0 | 3 | 10,00% |
| | | Prüfsumme | | | | | | | 100,00% |
| | | Summe | | | | | | | 5,83 |
| | | Summe | | | | | | | 6,49 |
| | | Summe | | | | | | | 6,69 |

Bewertungszahl von 0 - 10
 Bewertungszahl 0 entspricht Alternative erfüllt das Kriterium nicht
 Bewertungszahl 10 entspricht Alternative erfüllt das Kriterium vollständig

Fig. 20. Criteria Definition

2 means Criterion 1 is more important than Criterion 2
 1 means Criterion 1 is just as important as Criterion 2
 0 means Criterion 1 is less important than Criterion 2

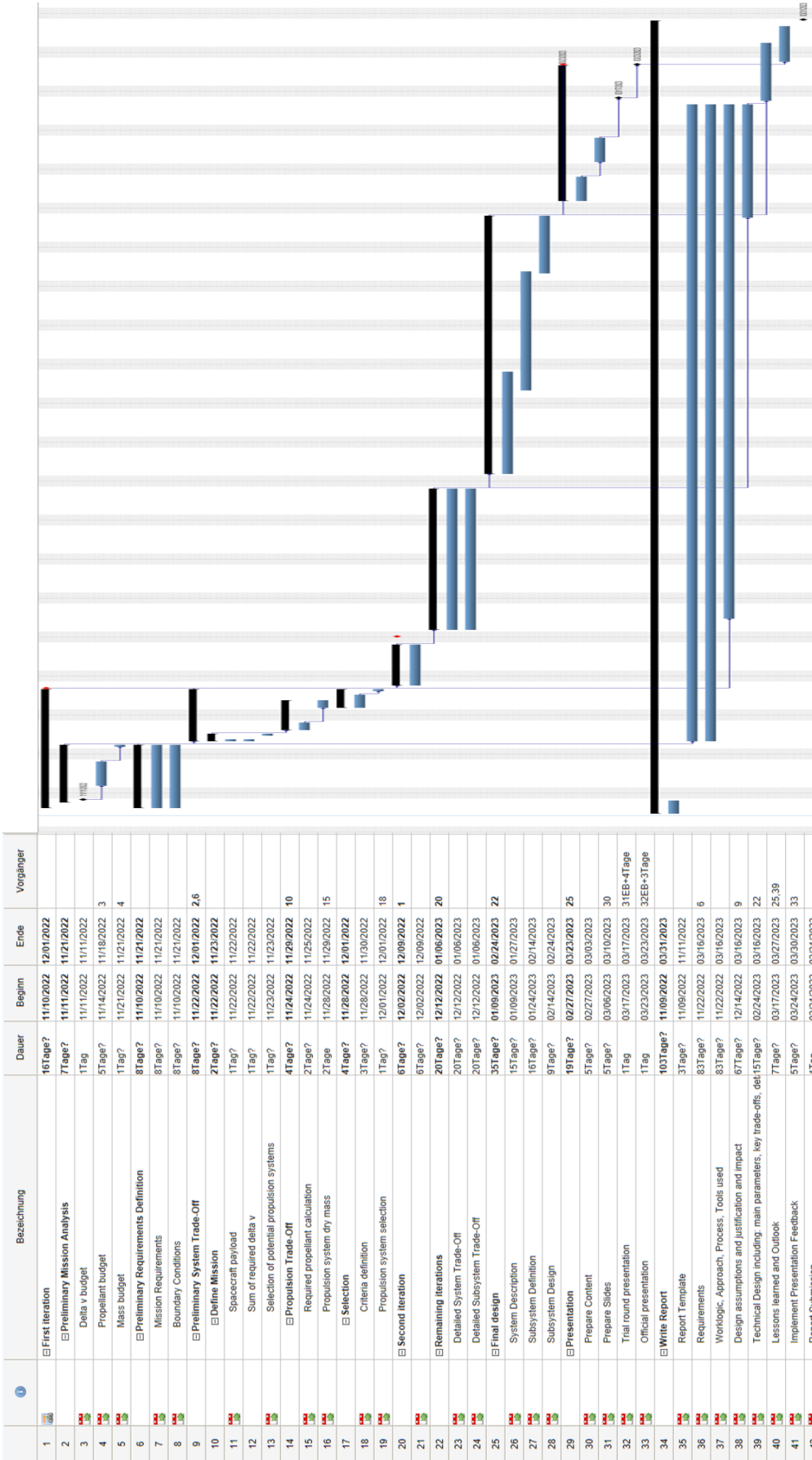


Fig. 21. MomentUM Project Plan

| Criterion | Background | Bipropellant (Aerojet) | Biprop Electric (Aerojet and Next_C) | Bipropellant (Ariane) | Biprop Electric (Ariane) |
|---------------------------------|------------------------------------|-------------------------------|---|------------------------------|---------------------------------|
| Propulsion system dry mass [kg] | m_PROP in MATLAB | 745,4764 | 0,0000 | 160,4047 | 8,9347 |
| Launch mass [kg] | m_prop in MATLAB + dry mass | 2,100,5286 | 0,0000 | 1,082,4001 | 10,0000 |
| Volume propulsion system [m3] | V_tot in MATLAB (Tank volumes * 3) | 3,4240 | 2,1256 | 2,2573 | 3,8127 |
| Power Requirement [W] | | 1,277,4168 | 10,0000 | 2,763,8654 | 8,5328 |
| Industrialization | European suppliers? | US | 0,0000 | US | 0,0000 |
| Technological risk | TRL | 9 | 10,0000 | 9 | 10,0000 |
| Toxicity of propellants | Hydrazine more toxic than MMH | Hydra/NTO | 0,0000 | Hydra/NTO and Xe | 0,0000 |
| | | | | MMH/NTO | 5,0000 |
| | | | | MMH/NTO and Xe | 5,0000 |

Fig. 22. Criteria Definition

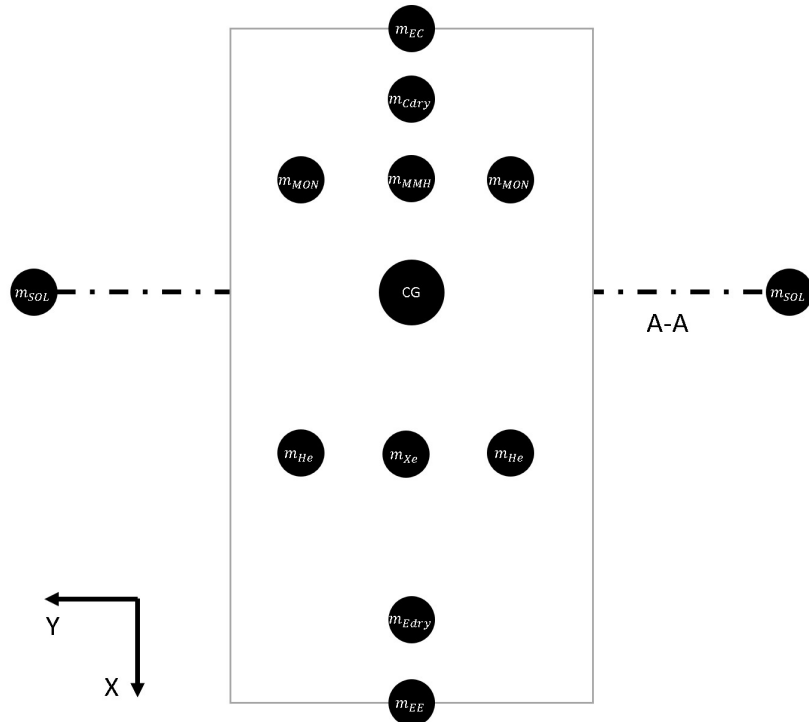


Fig. 23. Point-Mass Arrangement in the XY-plane

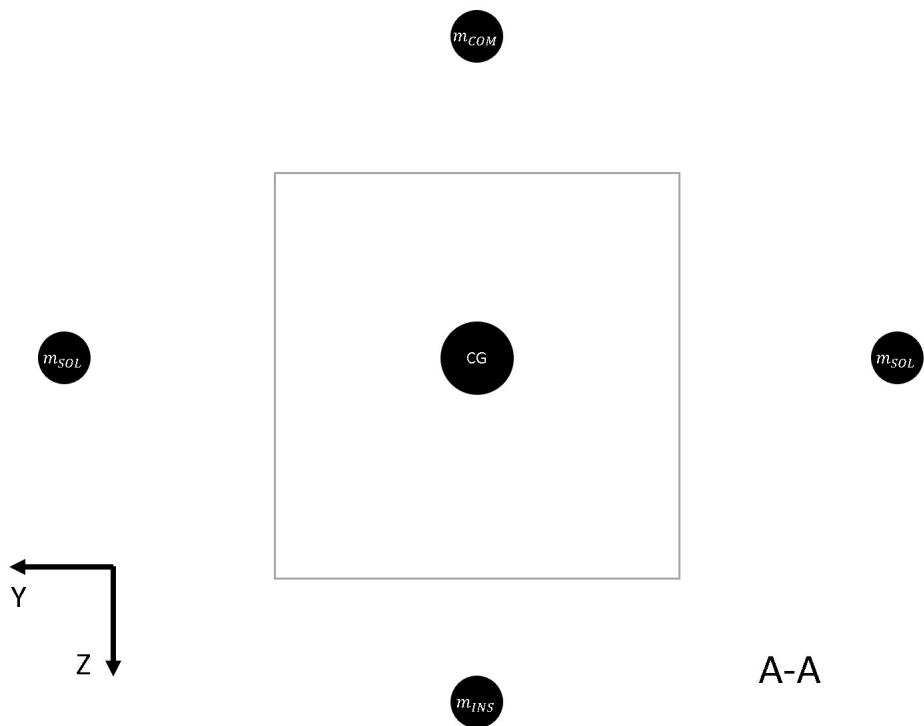
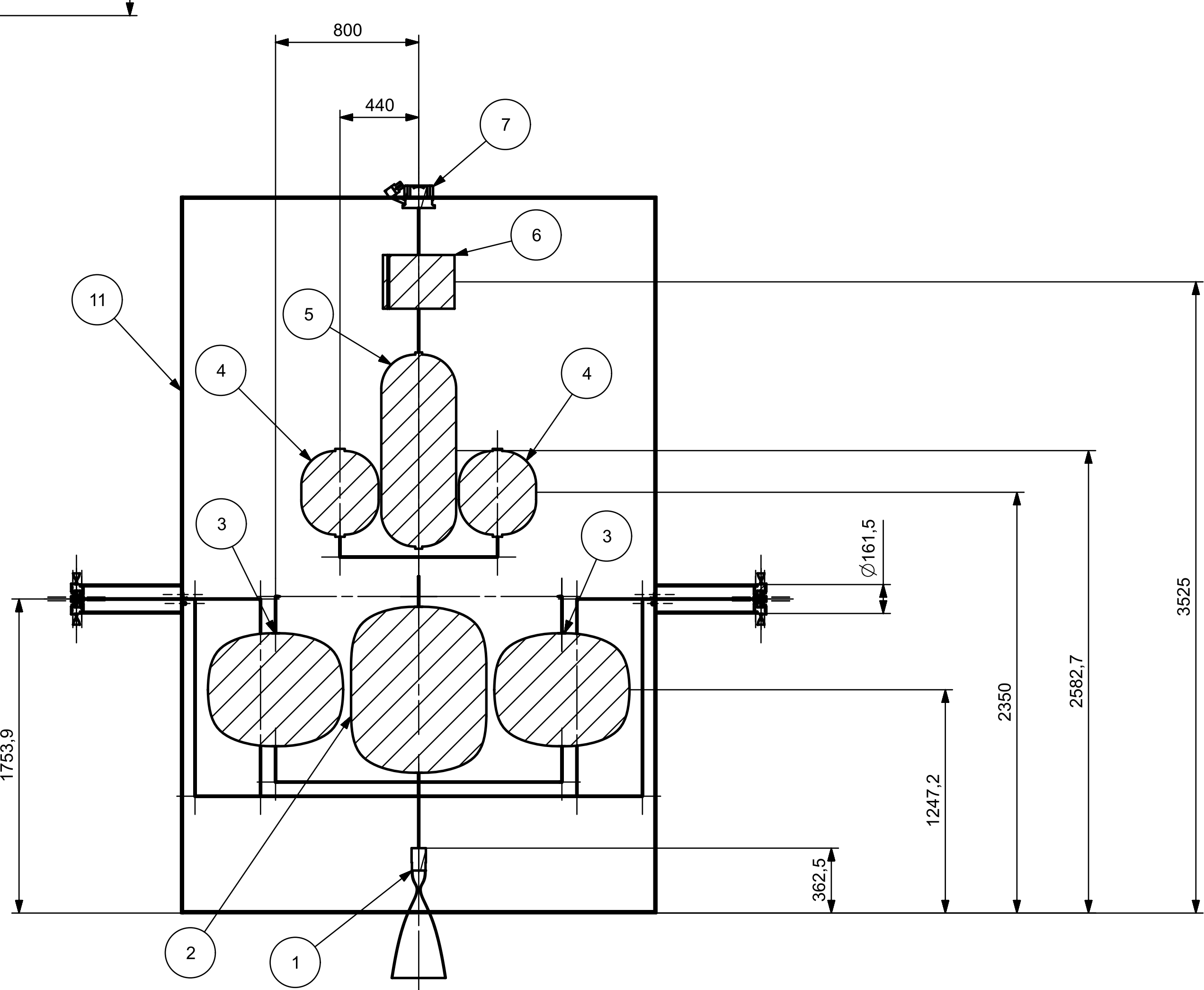
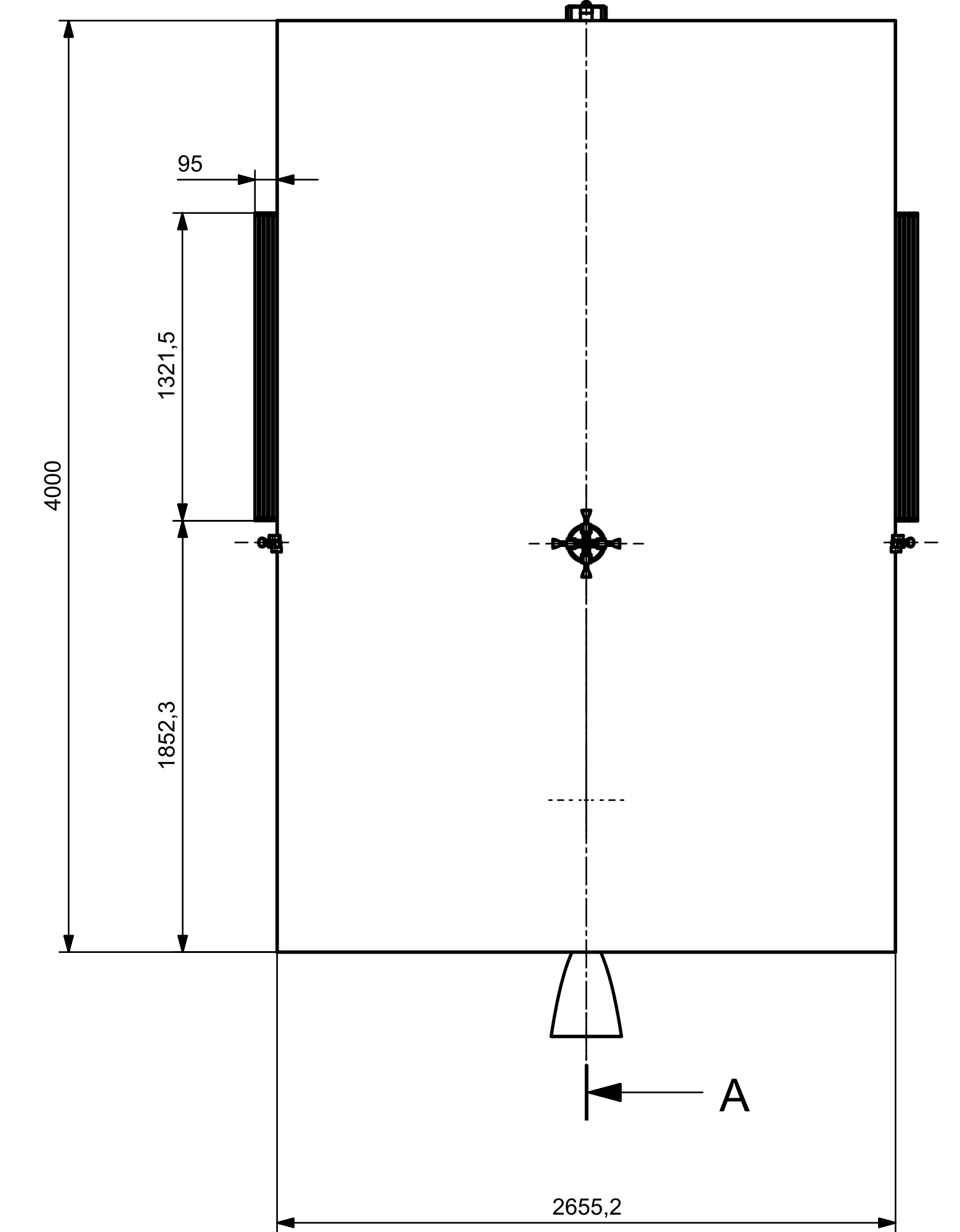
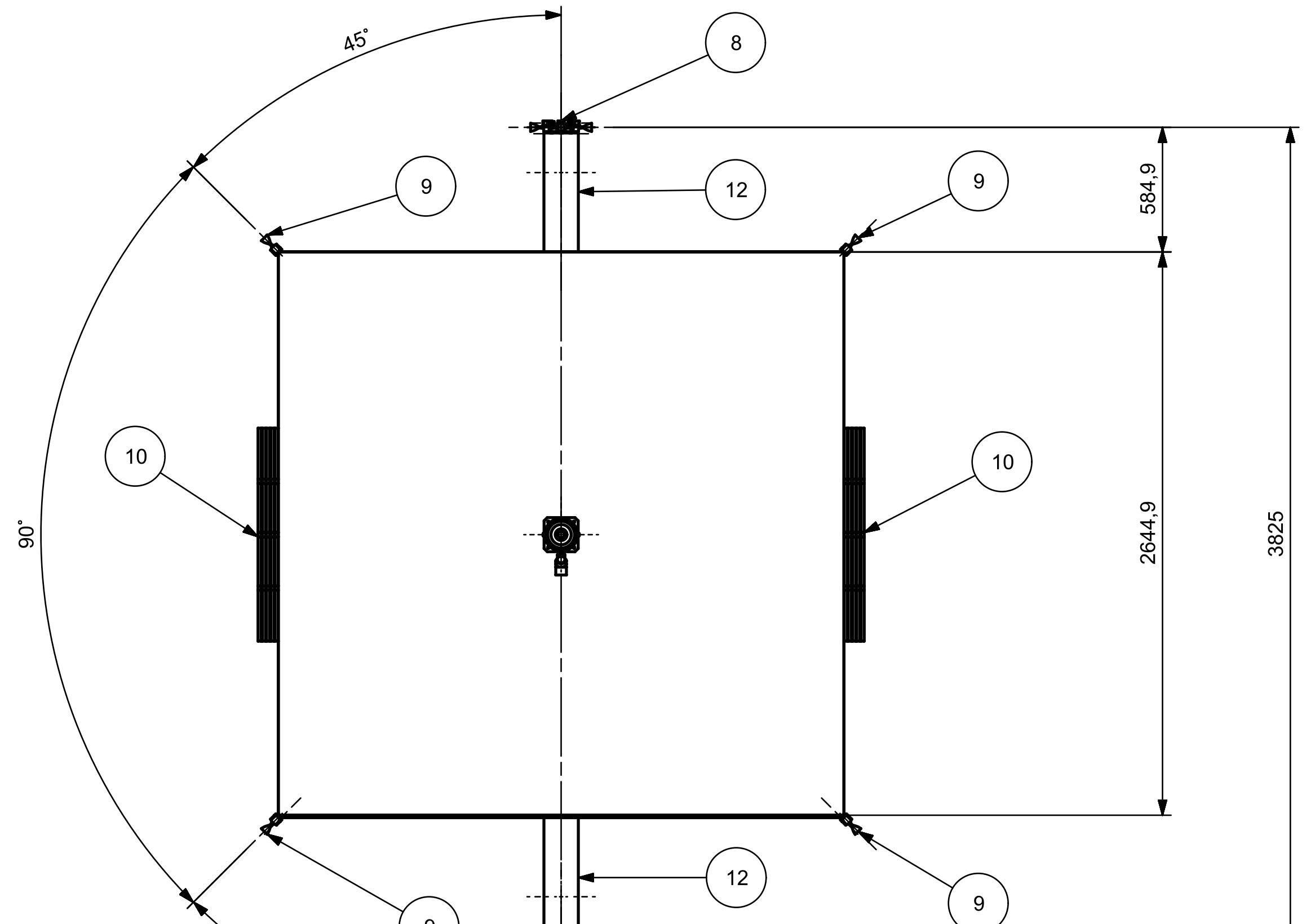
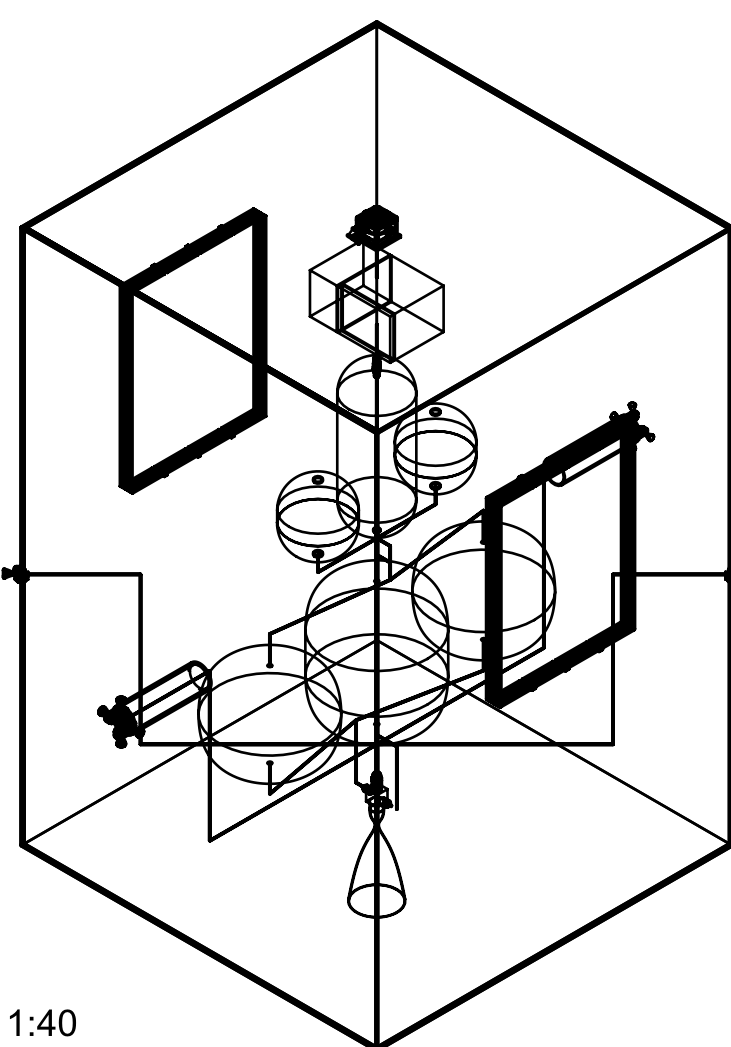
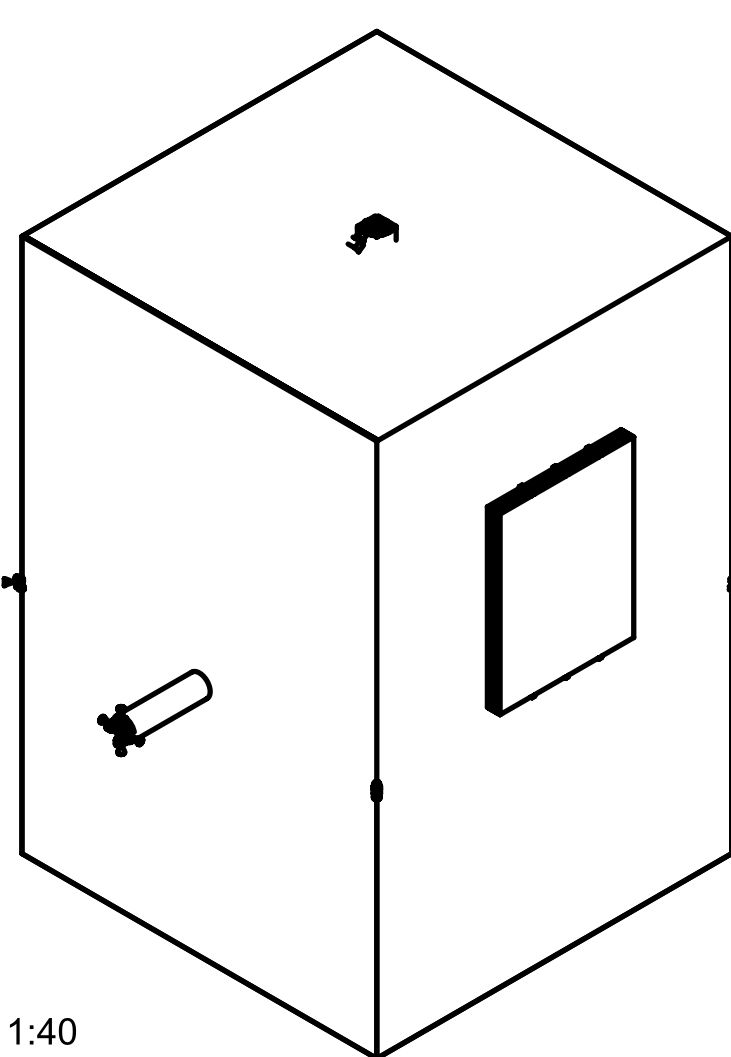


Fig. 24. Section of the Point-Mass Arrangement in the YZ-plane

MomenTUM

| Position | Part |
|----------|---|
| ① | ArianeGroup S400-15 bipropellant engine |
| ② | ArianeGroup OST 25/0 331L tank |
| ③ | ArianeGroup OST 25/0 198L tank |
| ④ | MT Aerospace PVG Family 40L tank |
| ⑤ | MT Aerospace S-XTA 120L tank |
| ⑥ | ETCA PPU, Safran BPRU, Safran XFC, EREAMS FU, Atermes PRE Card |
| ⑦ | Safran PPS 1350-G electric thruster |
| ⑧ | ArianeGroup S10-26 RCS thruster cluster |
| ⑨ | ArianeGroup S10-26 RCS thruster |
| ⑩ | Solar array (6.5 m x 1 m) |
| ⑪ | Spacecraft hull |
| ⑫ | RCS cluster connection |

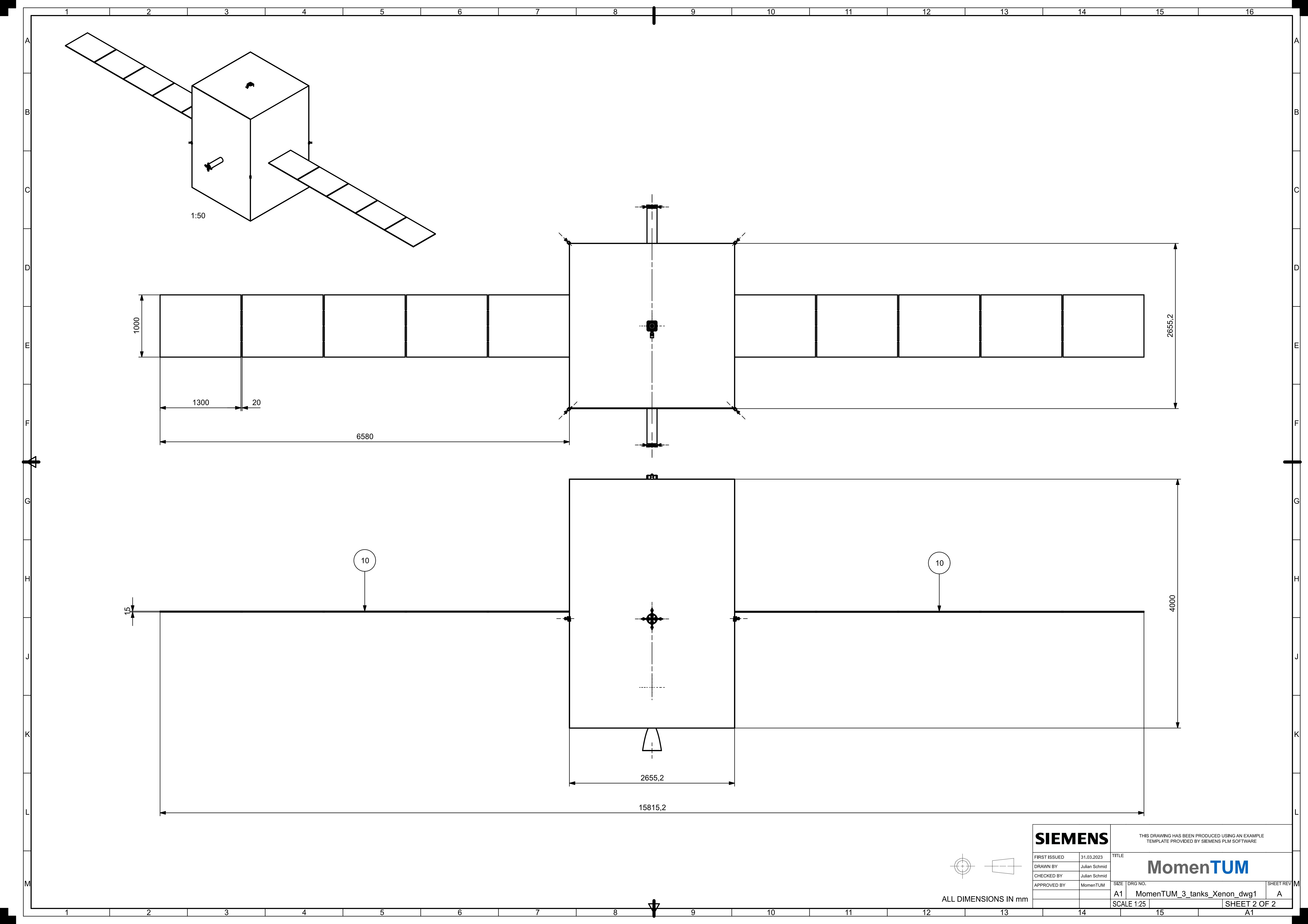


SECTION A-A

| | | | | |
|----------------|--|------------|-----------------------------|--|
| SIEMENS | THIS DRAWING HAS BEEN PRODUCED USING AN EXAMPLE TEMPLATE PROVIDED BY SIEMENS PLM SOFTWARE | | | |
| FIRST ISSUED | 31.03.2023 | TITLE | | |
| DRAWN BY | Julian Schmid | DRG NO. | | |
| CHECKED BY | Julian Schmid | SIZE | | |
| APPROVED BY | MomenTUM | SCALE 1:20 | MomenTUM_3_tanks_Xenon_dwg1 | |
| | | | A | |
| | | | SHEET REV M | |

ALL DIMENSIONS IN mm

SHEET 1 OF 2



SIEMENS

THIS DRAWING HAS BEEN PRODUCED USING AN EXAMPLE
TEMPLATE PROVIDED BY SIEMENS PLM SOFTWARE

FIRST ISSUED 31.03.2023

TITLE

DRAWN BY Julian Schmid

CHECKED BY Julian Schmid

APPROVED BY MomenTUM

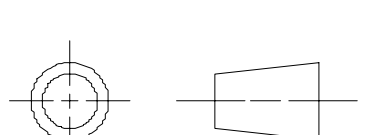
SIZE DRG NO.

A1 MomenTUM_3_tanks_Xenon_dwg1

SHEET REV M

SCALE 1:25

SHEET 2 OF 2



ALL DIMENSIONS IN mm

1 2 3 4 5 6 7 8 9 10 11 12 13 14 15 16

A B C D E F G H J K L M

A B C D E F G H J K L M

1 2 3 4 5 6 7 8 9 10 11 12 13 14 15 16

A B C D E F G H J K L M

A B C D E F G H J K L M

1 2 3 4 5 6 7 8 9 10 11 12 13 14 15 16

A B C D E F G H J K L M

A B C D E F G H J K L M

1 2 3 4 5 6 7 8 9 10 11 12 13 14 15 16

A B C D E F G H J K L M

A B C D E F G H J K L M

1 2 3 4 5 6 7 8 9 10 11 12 13 14 15 16

A B C D E F G H J K L M

A B C D E F G H J K L M

1 2 3 4 5 6 7 8 9 10 11 12 13 14 15 16

A B C D E F G H J K L M

A B C D E F G H J K L M

1 2 3 4 5 6 7 8 9 10 11 12 13 14 15 16

A B C D E F G H J K L M

A B C D E F G H J K L M

1 2 3 4 5 6 7 8 9 10 11 12 13 14 15 16

A B C D E F G H J K L M

A B C D E F G H J K L M

1 2 3 4 5 6 7 8 9 10 11 12 13 14 15 16

A B C D E F G H J K L M

A B C D E F G H J K L M

1 2 3 4 5 6 7 8 9 10 11 12 13 14 15 16

A B C D E F G H J K L M

A B C D E F G H J K L M

1 2 3 4 5 6 7 8 9 10 11 12 13 14 15 16

A B C D E F G H J K L M

A B C D E F G H J K L M

1 2 3 4 5 6 7 8 9 10 11 12 13 14 15 16

A B C D E F G H J K L M

A B C D E F G H J K L M

1 2 3 4 5 6 7 8 9 10 11 12 13 14 15 16

A B C D E F G H J K L M

A B C D E F G H J K L M

1 2 3 4 5 6 7 8 9 10 11 12 13 14 15 16

A B C D E F G H J K L M

A B C D E F G H J K L M

1 2 3 4 5 6 7 8 9 10 11 12 13 14 15 16

A B C D E F G H J K L M

A B C D E F G H J K L M

1 2 3 4 5 6 7 8 9 10 11 12 13 14 15 16

A B C D E F G H J K L M

A B C D E F G H J K L M

1 2 3 4 5 6 7 8 9 10 11 12 13 14 15 16

A B C D E F G H J K L M

A B C D E F G H J K L M

1 2 3 4 5 6 7 8 9 10 11 12 13 14 15 16

A B C D E F G H J K L M

A B C D E F G H J K L M

1 2 3 4 5 6 7 8 9 10 11 12 13 14 15 16

A B C D E F G H J K L M

A B C D E F G H J K L M

1 2 3 4 5 6 7 8 9 10 11 12 13 14 15 16

A B C D E F G H J K L M

A B C D E F G H J K L M

1 2 3 4 5 6 7 8 9 10 11 12 13 14 15 16

A B C D E F G H J K L M

A B C D E F G H J K L M

1 2 3 4 5 6 7 8 9 10 11 12 13 14 15 16

A B C D E F G H J K L M

A B C D E F G H J K L M

1 2 3 4 5 6 7 8 9 10 11 12 13 14 15 16

A B C D E F G H J K L M

A B C D E F G H J K L M

1 2 3 4 5 6 7 8 9 10 11 12 13 14 15 16

A B C D E F G H J K L M

A B C D E F G H J K L M

1 2 3 4 5 6 7 8 9 10 11 12 13 14 15 16

A B C D E F G H J K L M

A B C D E F G H J K L M

1 2 3 4 5 6 7 8 9 10 11 12 13 14 15 16

A B C D E F G H J K L M

A B C D E F G H J K L M

1 2 3 4 5 6 7 8 9 10 11 12 13 14 15 16

A B C D E F G H J K L M

A B C D E F G H J K L M

1 2 3 4 5 6 7 8 9 10 11 12 13 14 15 16

A B C D E F G H J K L M

A B C D E F G H J K L M

1 2 3 4 5 6 7 8 9 10 11 12 13 14 15 16

A B C D E F G H J K L M

A B C D E F G H J K L M

1 2 3 4 5 6 7 8 9 10 11 12 13 14 15 16

A B C D E F G H J K L M

A B C D E F G H J K L M

1 2 3 4 5 6 7 8 9 10 11 12 13 14 15 16

A B C D E F G H J K L M

A B C D E F G H J K L M

1 2 3 4 5 6 7 8 9 10 11 12 13 14 15 16

A B C D E F G H J K L M

A B C D E F G H J K L M

1 2 3 4 5 6 7 8 9 10 11 12 13 14 15 16

A B C D E F G H J K L M

A B C D E F G H J K L M

1 2 3 4 5 6 7 8 9 10 11 12 13 14 15 16

A B C D E F G H J K L M

A B C D E F G H J K L M

1 2 3 4 5 6 7 8 9 10 11 12 13 14 15 16

A B C D E F G H J K L M

A B C D E F G H J K L M

1 2 3 4 5 6 7 8 9 10 11 12 13 14 15 16

A B C D E F G H J K L M

A B C D E F G H J K L M

1 2 3 4 5 6 7 8 9 10 11 12 13 14 15 16

A B C D E F G H J K L M

A B C D E F G H J K L M

1 2 3 4 5 6 7 8 9 10 11 12 13 14 15 16

A B C D E F G H J K L M

A B C D E F G H J K L M

1 2 3 4 5 6 7 8 9 10 11 12 13 14 15 16

A B C D E F G H J K L M

A B C D E F G H J K L M

1 2 3 4 5 6 7 8 9 10 11 12 13 14 15 16

A B C D E F G H J K L M

A B C D E F G H J K L M

1 2 3 4 5 6 7 8 9 10 11 12 13 14 15 16

A B C D E F G H J K L M

A B C D E F G H J K L M